SDAC-TR-76-8

ON THE EXISTENCE, MAGNITUDE AND CAUSES OF BROAD REGIONAL VARIATIONS IN BODY-WAVE AMPLITUDES

ZOLTAN A. DER
Seismic Data Analysis Center
Teledyne Geotech, 314 Montgomery Street, Alexandria, Virginia 22314

19 May 1977

APPROVED FOR PUBLIC RELEASE; DISTRIBUTION UNLIMITED.

Sponsored by
The Defense Advanced Research Projects Agency (DARPA)
ARPA Order No. 2551

Monitored By
AFTAC/VSC
312 Montgomery Street, Alexandria, Virginia 22314

Unclassified

SECURITY CLASSIFICATION OF THIS PAGE (When Data Entered)

(14) **REPORT DOCUMENTATION PAGE**

READ INSTRUCTIONS BEFORE COMPLETING FORM

1. REPORT NUMBER: SDAC-TR-76-8 ✓	2. GOVT ACCESSION NO.
3. RECIPIENT'S CATALOG NUMBER	
4. TITLE (and Subtitle): (6) ON THE EXISTENCE, MAGNITUDE AND CAUSES OF BROAD REGIONAL VARIATIONS IN BODY-WAVE AMPLITUDES	5. TYPE OF REPORT & PERIOD COVERED: (4) Technical rept.
	6. PERFORMING ORG. REPORT NUMBER
7. AUTHOR(s): (10) Zoltan A. Der Der, Zoltan A.	8. CONTRACT OR GRANT NUMBER(s): (15) F08606-76-C-0004 ARPA Order-2551
9. PERFORMING ORGANIZATION NAME AND ADDRESS Teledyne Geotech 314 Montgomery Street Alexandria, Virginia 22314	10. PROGRAM ELEMENT, PROJECT, TASK AREA & WORK UNIT NUMBERS VT/6709
11. CONTROLLING OFFICE NAME AND ADDRESS Defense Advanced Research Projects Agency Nuclear Monitoring Research Office 1400 Wilson Blvd. Arlington, Virginia 22209	12. REPORT DATE: (11) 19 May 1977 13. NUMBER OF PAGES: 62 (12) 66 p.
14. MONITORING AGENCY NAME & ADDRESS (if different from Controlling Office) VELA Seismological Center 312 Montgomery Street Alexandria, Virginia 22314	15. SECURITY CLASS. (of this report): Unclassified 15a. DECLASSIFICATION/DOWNGRADING SCHEDULE

16. DISTRIBUTION STATEMENT (of this Report)

APPROVED FOR PUBLIC RELEASE; DISTRIBUTION UNLIMITED.

17. DISTRIBUTION STATEMENT (of the abstract entered in Block 20, if different from Report)

LPN-VT/6709

18. SUPPLEMENTARY NOTES

Author's Date 7 July 1976

19. KEY WORDS (Continue on reverse side if necessary and identify by block number)

Body-wave (m_b) — Partial Melting

Attenuation — M_s-m_b

20. ABSTRACT (Continue on reverse side if necessary and identify by block number)

This report is a review of evidence for anomalous attenuation of short-period seismic body-waves in the upper mantle under the Western United States. The attenuation reduces the amplitudes of these waves by a factor of about two relative to those observed in stable, continental shield type areas. The magnitude of this amplitude anomaly is consistent with spectral differences of body-waves observed in the same region, assuming a simple exponential attenuation law with a constant quality factor Q. The most likely cause of the attenuation is partial melting in the upper mantle under the Western United States. This hypothesis is → next page

DD FORM 1 JAN 73 1473 EDITION OF 1 NOV 65 IS OBSOLETE

Unclassified

SECURITY CLASSIFICATION OF THIS PAGE (When Data Entered)

408 258

supported by measurements of travel-time delays, upper mantle conductivity and heat flow. The report also includes a considerable number of new results obtained recently at the Seismic Data Analysis Center.

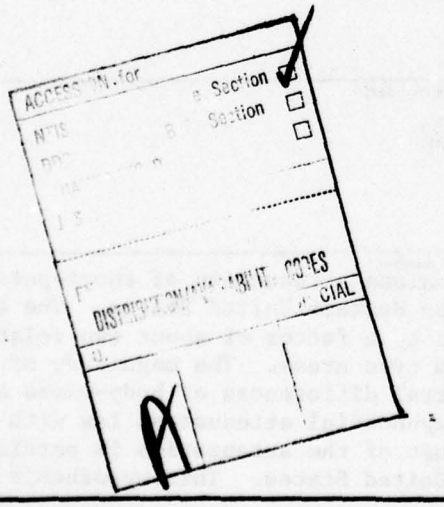

ON THE EXISTENCE, MAGNITUDE AND CAUSES OF BROAD REGIONAL VARIATIONS IN BODY-WAVE AMPLITUDES (MAGNITUDE BIAS)

SEISMIC DATA ANALYSIS CENTER REPORT NO.: SDAC-TR-76-8

AFTAC Project Authorization No.:	VELA T/6709/B/ETR
Project Title:	Seismic Data Analysis Center
ARPA Order No.:	2551
ARPA Program Code No.:	6F10
Name of Contractor:	TELEDYNE GEOTECH
Contract No.:	F08606-76-C-0004
Date of Contract:	01 July 1975
Amount of Contract:	$2,319,926
Contract Expiration Date:	30 June 1976
Project Manager:	Royal A. Hartenberger (703) 836-3882

P. O. Box 334, Alexandria, Virginia 22314

ABSTRACT

This report is a review of evidence for anomalous attenuation of short-period seismic body-waves in the upper mantle under the Western United States. The attenuation reduces the amplitudes of these waves by a factor of about two relative to those observed in stable, continental shield type areas. The magnitude of this amplitude anomaly is consistent with spectral differences of body-waves observed in the same region, assuming a simple exponential attenuation law with a constant quality factor Q. The most likely cause of the attenuation is partial melting in the upper mantle under the Western United States. This hypothesis is supported by measurements of travel-time delays, upper mantle conductivity and heat flow. The report also includes a considerable number of new results obtained recently at the Seismic Data Analysis Center.

TABLE OF CONTENTS

LIST OF FIGURES

LIST OF FIGURES (Continued)

LIST OF TABLES

INTRODUCTION

Many factors influence amplitudes of seismic waves from explosions and earthquakes. The identification of an explosion and estimation of its yield involve amplitude measurements on at least two kinds of waves (the P-wave arrival and the Rayleigh wave amplitude). In view of the recently proposed Threshold Test Ban Treaty (TTBT), which limits the yields of nuclear explosions, it is important to know how amplitudes of seismic waves depend on the region in which they were fired. There is a considerable amount of evidence that indicates that the amplitudes of waves at the teleseismic distance depend strongly on the geophysical properties of the source region. To estimate reliably the yield of explosions one must know the magnitude of such anomalies for each source region.

The body wave magnitude (m_b) is derived by the well-known formula

$$m_b = \log_{10}(A/T) + B(\Delta)$$

where A is the amplitude of the P-wave, T is its dominant period and B is a distance dependent, empirical term which approximately corrects for geometrical spreading and attenuation in an average Earth. All the quantities used in this formula strongly depend on transmission factors, many of which cannot be easily estimated, such as the velocity structure, variations in attenuation, receiver structure, etc. As a consequence, raw m_b values for any given event show a large scatter.

Not all of the factors influencing m_b for a given event will be discussed in this report. The effects of near source medium, device yield, source asymmetry, surface reflection or spall and near-surface geology are excluded from this discussion.

We also exclude the effects of multipathing and scattering from this discussion on the basis that such effects are essentially uncontrollable for single sites and extremely difficult to evaluate for arrays. One can assume that the scatter due to such effects can be reduced by taking averages of m_b over many stations. In this report we will examine broad regional differences in m_b values. Special attention will be given to the properties of the mantle under Nevada Test Site (NTS) as compared to other nuclear test sites.

An extensive review of the magnitude problem was given recently by Rodean (1976) who summarized all the relevant research to date. This report will show much of the illustrative material from the sources quoted by Rodean, and will discuss some relationships among various kinds of data as well as some discrepancies. Beyond qualitative geographical correlations between the various relevant geophysical parameters it will be shown that the observed P-wave amplitude variations are consistent with variations of Q in the upper mantle as deduced from spectral measurements of P-waves.

Rodean, H. C., 1976, Seismic yield verification and a regional M_s vs. m_b anomaly, Lawrence Livermore Laboratory, UCID-17006.

DIRECT EVIDENCE FOR THE EXISTENCE OF MAGNITUDE VARIATION FOR EVENTS IN WESTERN UNITED STATES (WUS) VS. EVENTS IN CONTINENTAL SHIELD AREAS (EUS IN PARTICULAR)

Many investigators have observed that the body-wave magnitudes for teleseismic events measured in the Western United States (WUS) differ from those measured in the Eastern United States (EUS) (Evernden and Clark, 1970; Booth, Marshall and Young, 1974; North, 1976). Body-wave magnitude measurements in the WUS were consistently 0.25 magnitude units lower than in the EUS. The average regional differences computed by other authors are in the range of 0.25-0.4 magnitude units. Figure 1 shows the magnitude terms for short-period P-waves at selected LRSM stations as determined from about 400 events by Booth, Marshall, and Young (1974). Although magnitude variations can have many causes, such as thick low-velocity sedimentary surface layers at the given stations, or focusing or defocusing of rays by local inhomogeneities, we shall see that the most plausible explanation of the general trend of short-period P-wave magnitude variations and associated phenomena in the WUS is anelastic attenuation due to a viscous, partially molten, low-velocity zone (LVZ) under the WUS.

Anelastic attenuation decreases the amplitude of a given frequency component of a wave by the factor:

$$\exp(-\pi f t^*)$$

where f is frequency, $t^* = t/Q_{av}$ where t is the travel time of a seismic wave and Q_{av} is the average quality factor along a given seismic ray. Since Solomons and Toksöz (1970) obtained lower Q values for long period waves than those deduced in this report the quality factor Q may be a function of frequency, but we shall assume it to be a constant between frequencies .5 and 4 Hz, the frequency band of short-period instruments used for measuring m_b. An effective

---

Evernden, J. and D. M. Clark, 1970, Study of teleseismic P. II. Amplitude data, Phys. Earth. Planet. Int., v. 4, p. 24-31.

Booth, D. C., P. D. Marshall, and J. B. Young, 1974, Long and short period amplitudes from earthquakes in the range 0°-114°, Geophys. J. R. Astr. Soc., v. 39, p. 523-538.

North, R. G. (1976) Station biases in body wave magnitude. (manuscript).

Solomon, S. C., and M. N. Toksöz, 1970, Lateral variation of attenuation of P and W waves beneath the United States, Bull. Seism. Soc. Am., v. 60, p. 819-838.

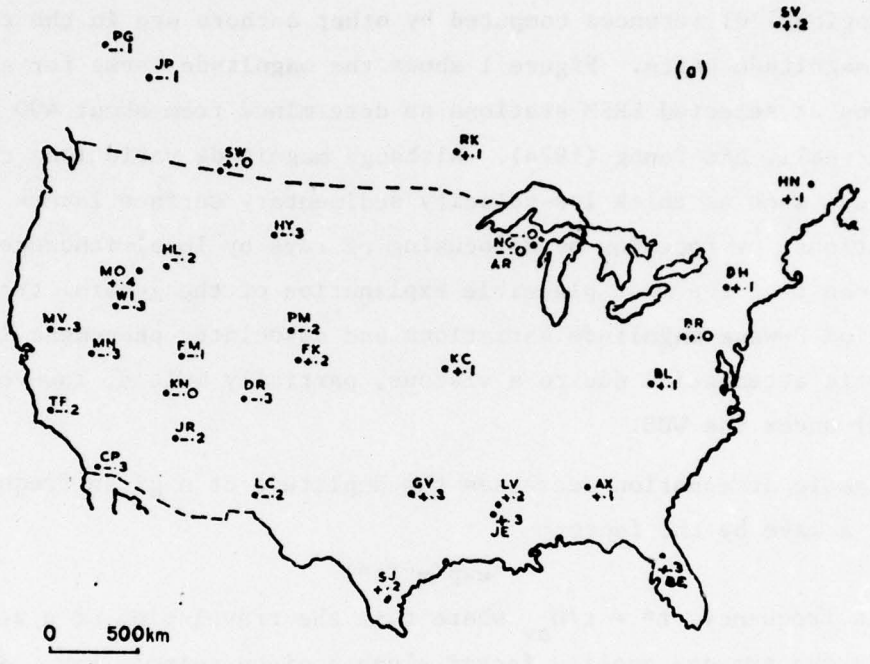

Figure 1. Short-period magnitude residuals based on the LRSM bulletin in the United States compiled by Booth, Marshall and Young, 1974.

value of t* can be measured directly by comparing the observed spectra of P-waves with that of the source, derived from close-in measurements (RDP). Relative differences of effective t* can be found by comparing the spectra at various stations.

If the observed magnitude variation is due to anelastic attenuation it has to be consistent with the t* values derived from spectral ratio measurements. A hot, partially molten upper mantle will lower the shear modulus of the material relative to a solidified cold mantle and lead to anelastic energy losses in shear deformation. This condition will reduce the S-wave amplitudes and velocities even more drastically than those of P-waves in the same frequency range. The values of anelastic t* for S-waves should be three to four times those for P-waves (Solomon and Toksöz, 1970). Anelastic attenuation as a cause of amplitude variation will also imply reciprocity, so that sources located in the WUS will seem to a distant observer to release less energy.

In Table I we show all estimates of effective t* values known to us at the present time. We include values from the literature as well as from our own research. In some cases we estimate t* from data or Q models published where t* was not stated explicitly. We also indicate the computational methods and assumptions used to derive t*, the epicentral distance range, and the nature of paths and sources. The model of Archambeau et al. (1969a,b) shows Q values which are too high relative to those derived by us in the Basin and Range, since the observed amplitude loss was interpreted in terms of a horizontally homogeneous model where the same Q model is assumed at source and receiver. The receivers in Archambeau's data are mostly in the high-Q EUS. In our interpretation of a causative LVZ practically all of the attenuation observed would be associated with a value only half of that computed by Archambeau et al. from a horizontally homgeneous model. The Q along the ascending paths reamins high. (The t* derived from a complete path through the Q model of Archambeau et al. is however a correct measure of the attenuation.)

The t* values in Table I range between -0.05 and 1. Shield type paths show lower values, while paths including the Basin and Range (BR) or tectonic

---

Archambeau, C. B., E. A. Flinn, and D. H. Lambert, 1969a, Fine structure of the upper mantle, J. Geophys. Res., v. 74, p. 5825-5865.

Archambeau, C. B., E. A. Flinn, and D. G. Lambert, 1969b, Detection, analysis and interpretation of teleseismic signals, 1. Compressional waves from the SALMON event, J. Geophys. Res., v. 73, p. 3877-3883.

TABLE I

EVENT TYPE, NAME, DATES	PATH	PATH TYPE	Δ°	Q_{AV}	t*	METHOD OBTAINED BY	SOURCE REFERENCE
NTS Nuclear Explosions	NTS-NORSAR	BR-S	73	1700	.41	Time domain waveform matching and spectral ratios	Frazier and Filson (1972)
NTS Nuclear Explosions	NTS-NPNT	BR-S	39	450	1.00	Time domain waveform matching	Trembly & Berg (1968)
NTS Nuclear Explosions	NTS- ?	BR-S?	21	543	.48†	Travel time & Amplitude studies	Archambeau, Flinn and Lambert (1968)
		BR-CP?	26	672	.50†		
			37	937	.46†		
NTS Nuclear Explosions	NTS-NORSAR	BR-S	73	--	.48**	Relative spectral ratios	Noponen (1975)
Misc. EQ's	Sakhalin-NORSAR	T-S	65-66	1800	.35	Spectral ratios to theoretical spectrum with ω^{-2} falloff rate at high frequencies	Noponen (1975)
Misc. EQ's	Kuriles-NORSAR	T-S	69	2900	.23		
Misc. EQ's	Central Asia-NORSAR	S-S	37-56	1900	.26		
Misc. EQ's	Crimea-NORSAR	T-S?	22-30	4400	.24		
Misc. EQ's	Greece-NORSAR	T-S	20-28	1200	.26		
Misc. EQ's	Turkey-NORSAR	T-S	23-30	840	.40		
Misc. EQ's	Italy-NORSAR	T-S	16-18	730	.33		
E. Kazakn Nuclear Explosions	E. Kazakh-NORSAR	S-S	38	2205	.20	Spectral ratios to von Seggern & Blandford theoretical spectrum	
Knickerbocker 26/05/67 NTS Nuclear Explosion	NTS-FKCO	BR-S	9.7	571	.25	Spectral ratios of observed P spectrum to the estimated source spectrum.	Der and McElfresh (1976b) [SDAC]
	-PGBC	BR-T	17.3	374	.65		
	-RKON	BR-S	21.2	585	.49		
	-WHYK	BR-T	26.2	925	.37		
	-HNME	BR-S	36.8	1254	.34		
	-SVQB	BR-S	37.8	964	.46		
	-NPNT	BR-S	39.1	1207	.37		
NTS Nuclear Explosions	NTS-EUS	BR-S	10-29	-	.75	Matching of amplitudes and waveforms of synthetic seismograms to actual data	Helmberger (1973)
USSR Explosions	Unspecified USSR	Unspecified mostly T?	10-32	710±150	.45-.69†††	Spectral ratio method	Berzon, Passechnik and Polikarpov
NTS Nuclear Explosions	NTS-SDCS Stations	BR-S			1.00	Matching amplitude and waveforms of synthetic seismograms to observations	Systems, Science and Software, Inc. Reports
USSR (Alma Ata) Earthquake	USSR Earthquakes to Yellowknife	S-S	80.0		.2	Matching amplitude and waveforms of synthetic seismograms to observations	Douglas et al. (1974)

TABLE I (Continued)

EVENT TYPE, NAME, DATES	PATH	PATH TYPE	Δ°	Q_{AV}	t*	METHOD OBTAINED BY	SOURCE REFERENCE
Piledriver, 02/06/66 NTS Nuclear Explosion	NTS-WNSD	BR-S	13.5	491	.40	Spectral ratios of observed P spectrum to the estimated source spectrum.	Der and McElfresh (1976b) [SDAC]
	-KCMO	BR-S	16.9	404	.59		
	-NPNT	BR-S	39.1	1250	.36		
Mast, 19/06/75 NTS Nuclear Explosion	NTS-RKON	BR-S	21.0	488	.58	Spectral ratios of observed P spectrum to the estimated source spectrum.	Der and McElfresh (1976b) [SDAC]
	-CPO	BR-S	24.7	476	.67		
	-WHYK	BR-T	26.2	420	.80		
	-FNWV	BR-S	28.9	546	.66		
	-HNME	BR-S	36.6	447	.96		
Gnome, 10/12/61 New Mexico Nuclear Explosion	N.M.-MPAR	S-S	9.3	1452	.09	Spectral ratios of observed P spectrum to the estimated source spectrum.	Der and McElfresh (1976b) [SDAC]
	-KNUT	S-CP	9.4	283	.48		
	-CWAR	S-S	10.3	1570	.10		
	-CPC1	S-T	10.6	603	.25		
	-WRAR	S-S	11.1	1701	.09		
	-WNSD	S-S	11.3	2092	.08		
	-JSTN	S-S	13.1	809	.23		
	-HLID	S-T	14.0	416	.48		
	-CVTN	S-S	14.1	1267	.16		
	-NGWS	S-S	18.1	1043	.25		
	-BLWV	S-S	19.3	1092	.24		
	-DHNY	S-S	25.0	1169	.28		
Salmon, 22/10/64 Mississippi Nuclear Explosion	Miss.-BLWV	S-S	9.5	∞	.00	Spectral ratios of observed P spectrum to the estimated source spectrum.	Der and McElfresh (1976a and b) [SDAC]
	-VOIO	S-S	11.3	2883	.06		
	-BRPA	S-S	12.4	6087	.03		
	-WFMN	S-S	12.8	515	.35		
	-RTNM	S-S	13.5	967	.20		
	-DHNY	S-S	16.1	1830	.12		
	-DRCO	S-CP	16.3	300	.77		
	-GPMN	S-S	16.8	2091	.11		
	-UBO	S-CP?	18.6	439	.59		
	-RKON	S-S	19.1	1169	.23		

TABLE I (Continued)

EVENT TYPE, NAME, DATES	PATH	PATH TYPE	Δ°	Q_{AV}	t*	METHOD OBTAINED BY	SOURCE REFERENCE
Salmon (Continued)	-KNUT	S-CP	20.1	434	.64		
	-EKNV	S-BR	22.8	690	.44		
	-SBQB	S-S	28.7	1566	.23		
	-NPNT	S-S	47.3	2203	.23		
N. Zemlya Explosion 25/10/64	N. Zemlya-SVQB*	S-S	45.8		-.05††	Relative spectral ratios	Der & McElfresh [SDAC]
	-RKON	S-S	54.0		-.08††		
	-HNME	S-S	54.2		.11††		
	-LSNH	S-S	56.9		.16††		
	-WFMN*	S-S	60.7		.09††		
	-VOIO*	S-S	62.2		-.01††		
	-EKNV	S-BR	67.4		.34††		
	-DRCO	S-CP	68.6		.07††		
	-RTNM	S-S	69.0		.08††		
	-KNUT	S-CP	69.4		-.03††		
	-NLAZ	S-CP	70.3		.03††		
	-GEAZ	S-BR	72.5		.36††		
	-LCNM	S-BR	73.5		.01††		
N. Zemlya Explosion 21/10/67	N. Zemlya-SVQB*	S-S	45.8		.04††	Relative spectral ratios	Der & McElfresh [SDAC]
	-WHYK	S-T	46.0		.22††		
	-PGBC	S-T	52.8		.25††		
	-RKON*	S-S	54.0		.01††		
	-HNME	S-S	54.2		.17††		
	-HVMA	S-S?	57.9		.28††		
	-WNSD*	S-S	62.2		-.04††		
	-HLID	S-T	63.0		.13††		
	-KNUT	S-CP	69.4		.14††		
	-LCNM	S-BR	73.5		.41††		

Legend

* stations used in computing an average reference spectrum
** relative to E. Kazakh values
† implied by their velocity and Q model
†† t* values relative to the average of stations marked by stars
††† assuming negligible attenuation in the Depth range 0-100 km.

Abbreviations

S shield (stable platform)
T tectonic (general)
CP Colorado plateau
BR Basin and range

TABLE Ia,b

WUS-EUS

	Δ°	t*	
NTS - FKCO	9.7	.25	KNICKERBOCKER
NTS - RKON	21.2	.49	
NTS - WNSD	13.5	.40	PILEDRIVER
NTS - KCMO	16.5	.59	
NTS - RKON	21.0	.58	MAST
NTS - CPO	24.7	.67	
NTS - FNWV	28.9	.66	
N. Mexico - KNUT	9.4	.48	GNOME
N.M - CPCL	10.6	.25	
N.M - HLID	14.0	.48	
Miss. - DRCO	16.3	.77	SALMON
Miss. - UBO	18.6	.59	
Miss. - KNUT	20.1	.64	
Miss. - EKNU	22.8	.44	
	17.7	.52	

14 values

Table Ia,b (Continued)

EUS

	Δ°	t*	
N.M. - MPAR	9.3	.09	GNOME
N.M. - CWAR	10.3	.10	
N.M. - WRAR	11.1	.09	
N.M. - WNSD	11.3	.08	
N.M. - JSTN	13.1	.23	
N.M. - CVTN	14.1	.16	
N.M. - NGWS	18.1	.25	
N.M. - BLWV	19.3	.24	
N.M. - DHNY	25.0	.28	
Miss. - BLWV	9.5	.00	SALMON
Miss. - VDIO	11.3	.06	
Miss. - BRPA	12.4	.03	
Miss. - WFMN	12.8	.35	
Miss. - RTNM	13.5	.20	
Miss. - DHNY	16.1	.12	
Miss. - GPMN	16.8	.11	
Miss. - RKON	19.1	.23	
Miss. - SVQB	28.7	.23	
Avg.	15.1	.158	

18 values

(T) path segments are higher. We purposely excluded from Table I t* (or Q) values published for paths including island arc or oceanic ridge segments. Instead, we center our discussion on relative differences between the WUS and the EUS or, in a broader sense, between pure shield (stable platform) type paths and paths which include a segment of the Basin and Range province.

We have computed a large number of effective t* values by dividing the spectra of the first nine seconds of the P-wave signal at various LRSM stations with estimated explosion source spectra which were derived from scaling of close-in seismic measurements (Von Seggern and Blandford, 1972). These t* values compare well with the other t* values published or implied by other authors in Table I. The scatter is not great considering that we are dealing with short-period data, and that the t* values listed were derived by various methods.

The t* values for the $9° < \Delta < 36°$ distance range are more likely to be influenced by differences in the crust-upper mantle velocity structure due to travel time triplications and crustal guided waves than those for greater distances. It is unlikely, however, that such influences are very important for relative t* estimates. What we are measuring, in effect, is the rate of fall-off of the spectra at high frequencies. Travel time triplications, crustal response, multipathing and other often quoted factors may modulate the spectrum by introducing nulls and maxima, especially at shorter epicentral distances (the values in Table I with $9° < \Delta < 36°$), but they cannot explain the uniform removal of high-frequency energy within the seismic pass band. Seismograms at the same epicentral distances have similar envelopes due to the same upper mantle triplications of travel times associated with the steep gradients at the 400 and 600 km depths that are identical for the WUS and EUS reference, but the frequency content of the seismograms is quite different due to the different attenuations along the various paths.

The effect is visibly quite dramatic on seismograms for small explosions where the source spectrum is nearly flat within the frequency range studied (the SALMON and GNOME nuclear explosions, for example). For these events the 3-4 Hz energy is almost completely absent at stations with $\Delta > 9°$ along EUS-WUS paths, while it is conspicuously present along pure EUS (shield) type paths. (Der and McElfresh, 1976a) The effect is still visible to the eye but less obvious for larger explosions where most of the energy is at frequencies

f < 1.5 Hz, but spectral analysis shows that the falloff rate at higher frequencies is considerably steeper for EUS-WUS type paths in all cases (Der and McElfresh, 1976b).

Because of the method of analysis employed here, the effects of surface reflections are also small. For each explosion used in determining t* we assessed the possible effect of a linear superposition of pP; in all the cases we analyzed, it seemed to be minor for at least one of the following reasons:

a) There are no obvious nulls in the spectra which can be associated with pP (most common case), or the surface reflection coefficient is small;
b) The spectral ratio straight-line fit covers several nulls and maxima, thus smoothing out the pP effect;
c) The fit is over one maximum (which should give zero slope with small attenuation and a flat source spectrum), but lobes at higher frequencies are missing, indicating high t*; and
d) We determined relative t* values in which case the source spectrum and its modulation are irrelevant.

Next we will show that the observed magnitude variations are consistent with the differences in effective t* as determined from spectral ratios. We first discuss t* values determined by SDAC for sources between the epicentral distance $9° < \Delta < 35°$. We classify all t* values from North America into two groups: "EUS" type paths which are entirely under the eastern, tectonically stable part of the continent, and "mixed" EUS-WUS paths which cross into the WUS. Histograms constructed for these two groups are shown in Figure 2. is a clear separation between the t* values of the two groups. The mean t* for EUS-type paths is 0.16, and for mixed paths it is 0.52. The data in both groups cover the same distance-travel time range.

Figure 3 shows a plot of relative magnitudes (observed m_b - log(yield)) of GNOME and SALMON at various LRSM stations vs. t* at these stations. Magnitude is proportional to log(A/T). (Blandford, 1976; and Werth and Herbst, 1963) There is a considerable amount of scatter, but the amplitudes tend to

---

Blandford, R. R., 1976, Experimental determination of scaling laws for contained and cratering explosions, SDAC-TR-3, Teledyne Geotech, Alexandria, Virginia. ADA 03635

Werth, G. C., and R. F. Herbst, 1963, Comparison of amplitudes of seismic waves from nuclear explosions in four mediums, J. Geophys. Res., v. 68, p. 1463-1475.

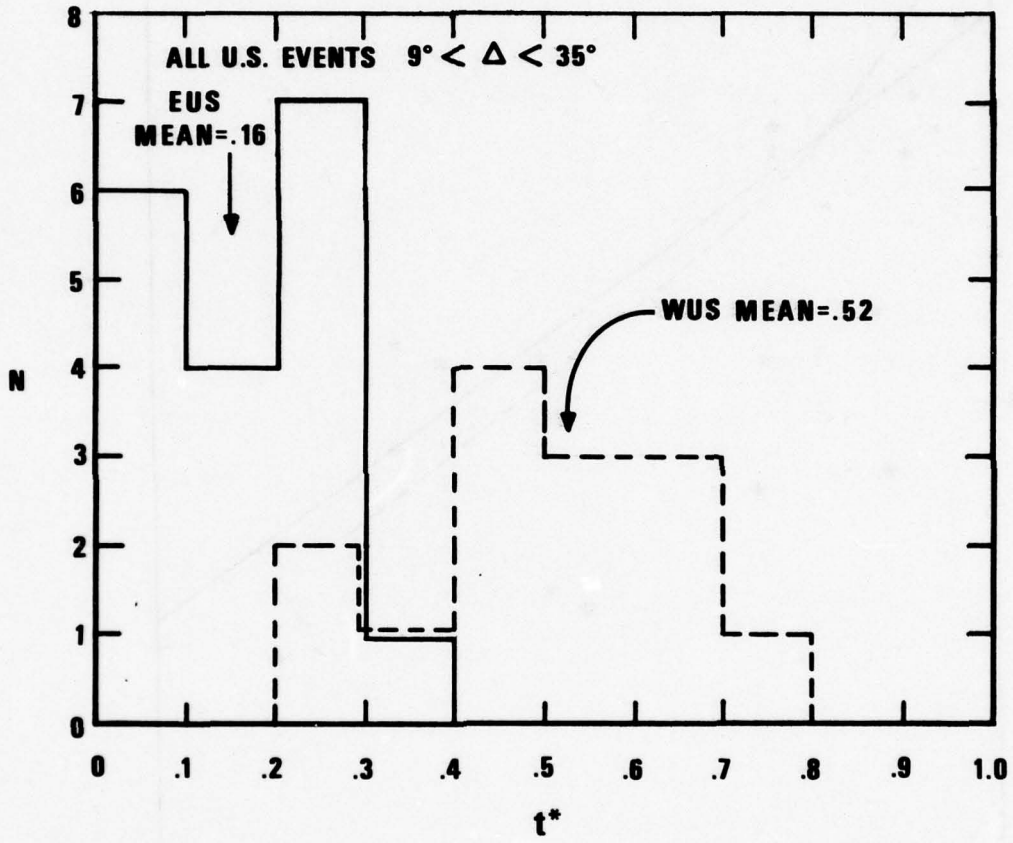

Figure 2. Summary of 9° < Δ < 35° t* values classified with respect to EUS and mixed path types. Der and McElfresh (1976).

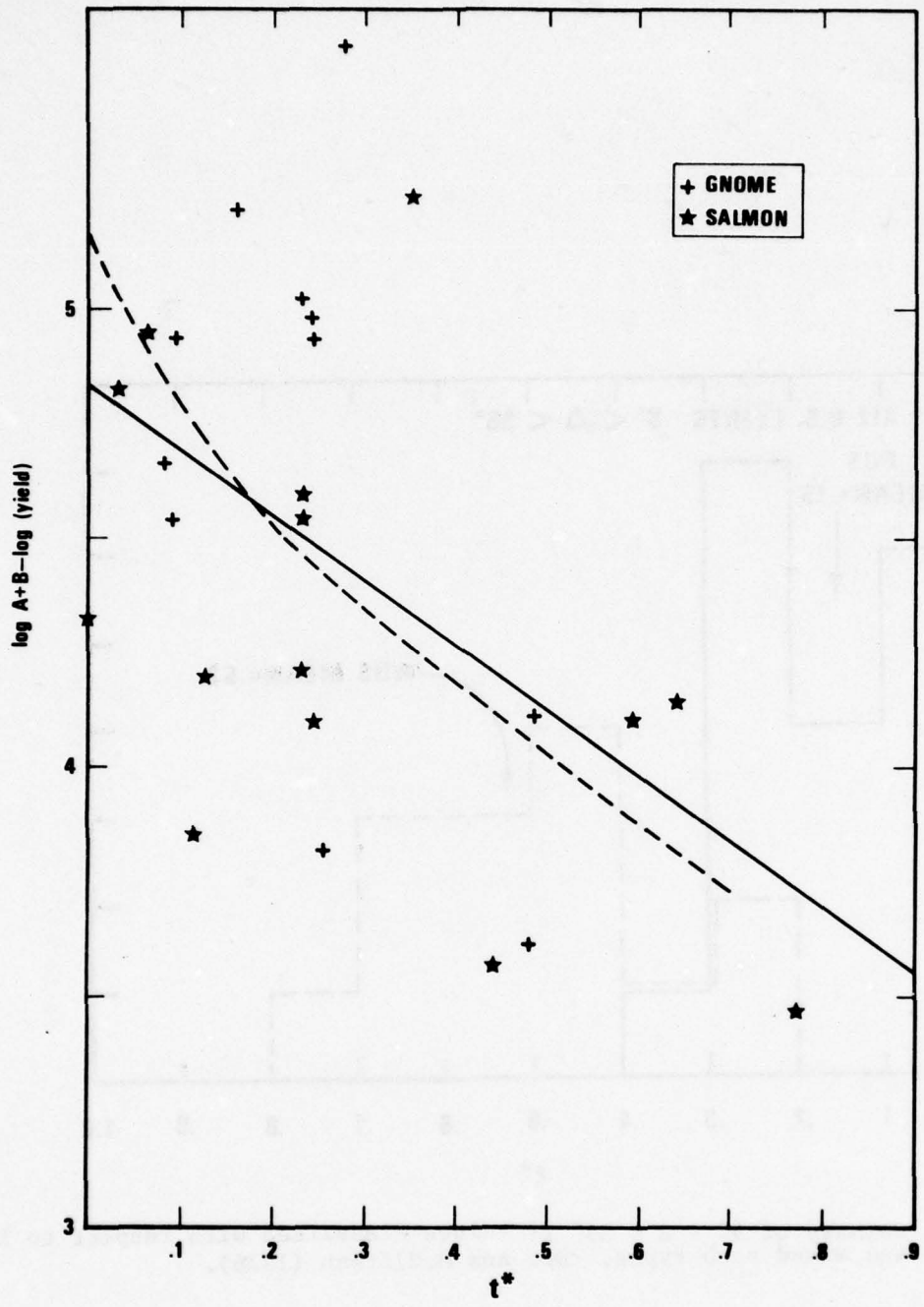

Figure 3. Reduced magnitudes from explosions GNOME and SALMON as functions of t*. Solid line corresponds to the amplitude factor $\exp(-\omega t^*/2)$ for f = 1 Hz. Der and McElfresh (1976b). Dashed line gives the theoretically calculated log(A/T) with A corrected for LRSM system response at period T for a 5 kiloton explosion in salt using the reduced displacement potential of GNOME from Werth and Herbst (1963) and the calculation techniques from Blandford (1976).

decrease with increasing t*. The slope of the solid line drawn corresponds to $\exp(-\pi t^*)$, the attenuation factor at f = 1, the actual falloff with t* is greater because the dominant frequency of P-wave is greater than 1 Hz for these events. The dashed line shows this in more detail. It is calculated by the methods of Blandford (1976). Theoretical waveforms are calculated and the maximum peak-to-peak amplitude is measured. The interval between zero-crossings on either side of the maximum peak-to-peak excursion is taken as the period T, and A is then the measured amplitude corrected for the system response at period T. (Both lines have been shifted vertically to fit the observed absolute level of the data visually.) This was done because we have not performed the complete calculations necessary to predict the absolute level of the signals from a specified yield. Regression analysis shows that slope zero can be rejected with > 99% confidence and that about half of the observed variance in m_b is due to t*.

The outlying points on Figure 3 do not necessarily represent large fluctuations in m_b alone. Errors in t* measurement also contribute to the scatter.

Figure 4 shows histograms of t* values at teleseismic distance $\Delta > 35°$. The t* values used in this histogram are summarized in Tables II and III. We have included all published t* values known to us as well as our own. Relative t* values for Novaya Zemlya events (Novaya Zemlya is known to be on a stable platform (Molnar and Oliver, 1969) were also included by adding a constant to all relative values to make the average t* of shield paths equal. We subdivided the associated wave paths into two groups: the paths which start and end in tectonically stable regions (shield in an extended sense) and those that have one end (ascending or descending) in the Basin and Range province while the other end of the raypath is in a shield region. The difference in means is 0.31. In the average of the shield to WUS paths we included two extremely high t* values, the Mast-HNME and the Trembly and Berg t* determinations. If we exclude these as outliers, the difference between the mean t* of the two populations becomes $\delta t^* = 0.23$. Making a rough adjustment for the differences in the average epicentral distances represented in the two groups (about 10°) by multiplying δt^* with the ratio of travel times at the mean epicentral distances the adjusted δt^* becomes 0.21.

Calculations using a granite reduced displacement potential for 100 kt in Blandford (1976) shows that as t* varies between 0.2 and 0.4, and assuming no surface reflection, log(A/T) varies 0.30 magnitude units. This corresponds well to the magnitude differences tabluated by Booth et al. (1975).

In comparing t* values for paths to stations KNUT, DRCO and NLAZ in the Colorado Plateau province, there seems to be an indication of a directional

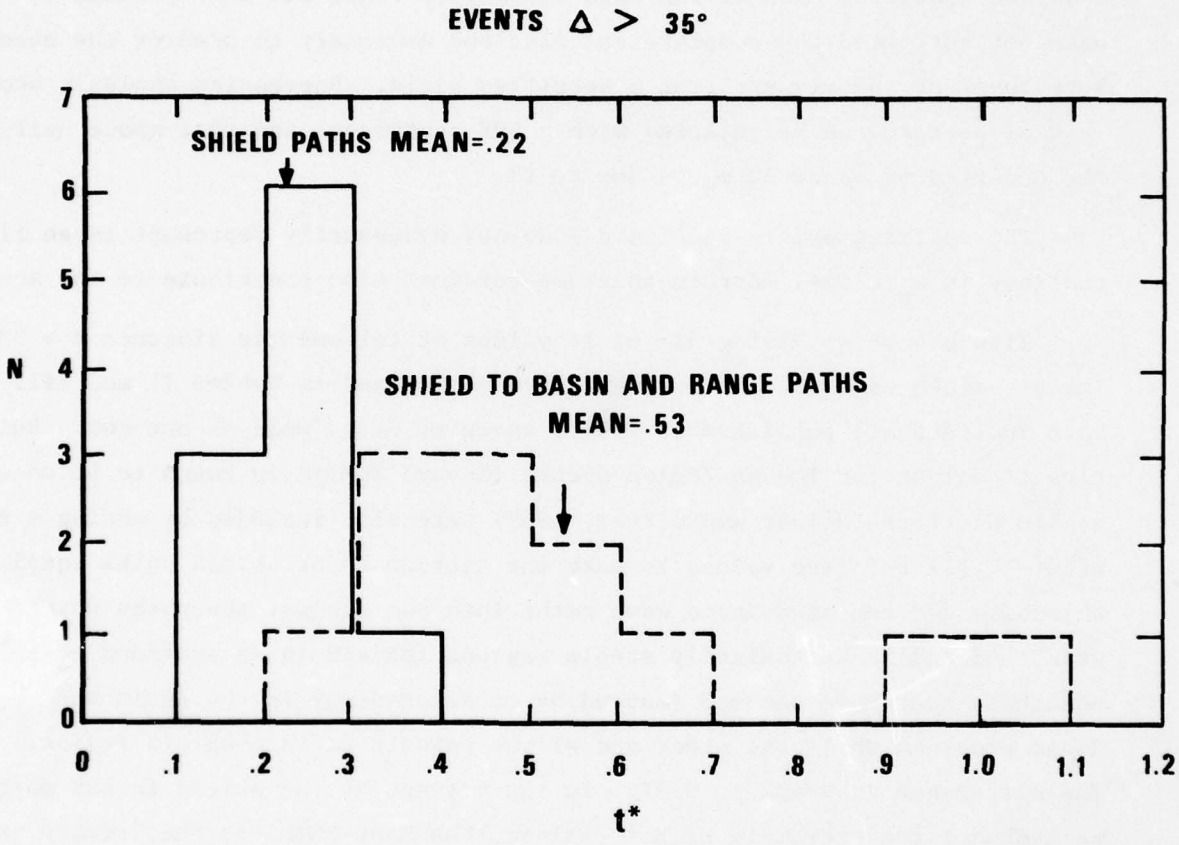

Figure 4. Summary of t* values for Δ > 35°, listed in Tables II and III.

TABLE II

SHIELD AND STABLE PLATFORM PATHS FOR $\Delta > 35°$

		$\Delta°$	t*
Central Asia - NORSAR	(Noponen, 1975)	36 - 37	.26
E-Kazakh - NORSAR	(Noponen, 1975)	38.0	.20
Salmon - NPNT	SDAC	47.3	.23
N. Zemlya - RKON	SDAC	54.0	.15+
N. Zemlya - SV2QB	SDAC	45.8	.18+
N. Zemlya - VOIO	SDAC	62.0	.24+
N. Zemlya - WFMN	SDAC	60.7	.32+
N. Zemlya - RKON	SDAC	54.0	.24+
N. Zemlya - SV3QB	SDAC	45.8	.23+
N. Zemlya - WNSD	SDAC	62.2	.19+
		Average	.22

+ adjusted relative measurements

TABLE III

MIXED (SHIELD AND STABLE PLATFORM TO BASIN & RANGE) PATHS

		Δ°	t*
NTS - NORSAR	Frazier-Filson, 1972	∿70	.41
NTS - NORSAR	Noponen, 1975	∿70	.48
Mast - HNME	SDAC	∿36.6	.95
Piledriver - NPNT	SDAC	39.9	.36
Knickerbocker - SV3QB	SDAC	37.8	.456
Knickerbocker - NPNT	SDAC	39.1	.373
Knickerbocker - HNME	SDAC	36.7	.344
NTS - NPNT	Trembly-Berg	39.0	1.00
N. Zemlya - EKNV	SDAC	67.4	.57+
N. Zemlya - GEAZ	SDAC	72.5	.59+
N. Zemlya - LCNM	SDAC	73.5	.24+
N. Zemlya - LCNM	SDAC	73.5	.64+
		Average	.53

+ adjusted relative measurements

dependence in t*. P-waves from the SALMON explosion seem to be attenuated while those coming from Novaya Zemlya are not. A possible explanation is that waves coming from the direction of Novaya Zemlya emerge under the Plateau while those coming from the Southeast cross part of the partially molten upper mantle region which is characteristic of the Basin and Range and Front Ranges and which possibly extends under the southern edge of the plateau. The Colorado Plateau itself is characterized by low heat flow, low conductivity (see the map of Gough, Figure 20) and, quite likely, colder and less attenuating mantle (Roy et al., 1972). Table IV gives a summary of t* values for SALMON and Novaya Zemlya shots recorded in the Colorado Plateau. We have only a few values and the matter might well be investigated further. Spectra of Novaya Zemlya shots from signals recorded at stations in the Basin and Range and elsewhere in the WUS seem to indicate higher attenuation than for the Colorado Plateau stations.

To analyze the Novaya Zemlya explosions further, we have assumed that the magnitude vs. t* dependence is linear and has the same slope for all events resulting in an equation of the form:

$$\overset{m}{n}m = a_n + bt^*_m$$

at station m and for event n. We estimated all a_n by regression analysis and subtracted them from the m_b's associated with each event to make the plot found in Figure 5. This figure is similar to Figure 3. The common slope (b) was also estimated and found to be -1.93 ± 1.14 (95% confidence limits). The probability of zero slope, which would be equivalent to no functional dependence of m_b's on t*, is less than 1%.

The 95% confidence range for the slope includes the value -1.50 which would give 0.3 m_b difference for a Δt^* of 0.2. As we saw above, this is the difference which would be predicted as t* varies from 0.2 to 0.4 for a 100 kt shot in granite as recorded at an LRSM station.

Similar differences in spectral content of P-waves exist in other areas

---

Roy, R. F., D. D. Blackwell, and E. R. Decker, 1972, Continental heat flow. The Nature of the Solid Earth (E. C. Robertson, Editor), McGraw Hill International Series in the Earth and Planetary Sciences.

TABLE IV

COLORADO PLATEAU t* VALUES

From SALMON		From N. Zemlya	
Station	t*	Station	t*
UBO	.592	KNUT	.36
KNUT	.639	KNUT	.18
DROC	.769	NLAZ	.25
		DRCO	.29
Average	.66	Average	.27

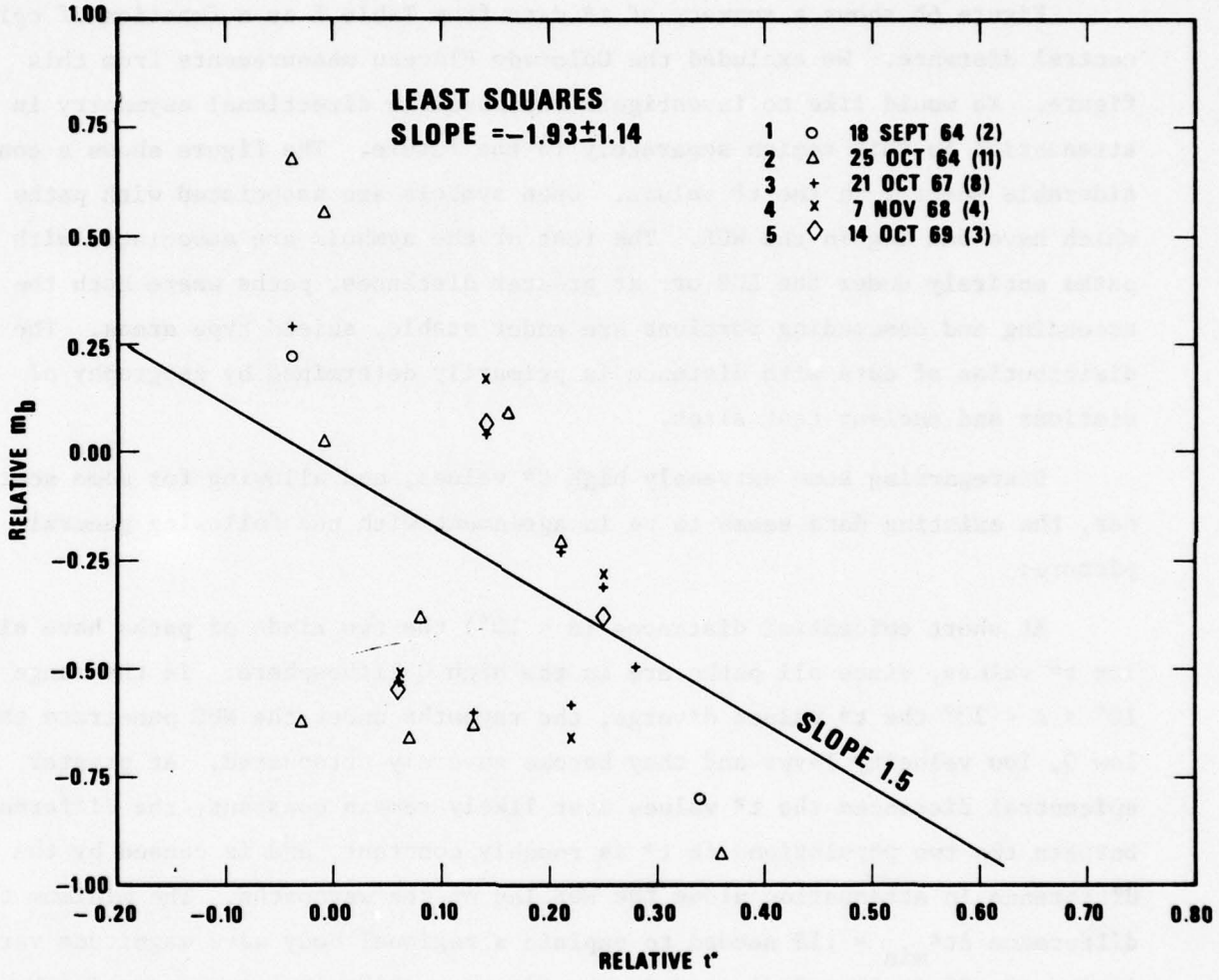

Figure 5. Relative m_b plotted against relative t* for five Novaya Zemlya events.

of the world. Figure 6a shows a figure from a report by Noponen showing the LTM discriminant (normalized third moment of the amplitude spectrum) at NORSAR for explosions in various regions of the world (black dots). Paths to NTS give low LTM values indicating the lack of high frequencies. Note that data from earthquakes (open symbols) behave in the same way.

Figure 6b shows a summary of t* data from Table I as a function of epicentral distance. We excluded the Colorado Plateau measurements from this figure. We would like to investigate the possible directional asymmetry in attenuation in this region separately in the future. The figure shows a considerable scatter in the t* values. Open symbols are associated with paths which have one leg in the WUS. The rest of the symbols are associated with paths entirely under the EUS or, at greater distances, paths where both the ascending and descending portions are under stable, shield type areas. The distribution of data with distance is primarily determined by geography of stations and nuclear test sites.

Disregarding some extremely high t* values, and allowing for some scatter, the existing data seems to be in agreement with the following general picture:

At short epicentral distances ($\Delta < 10°$) the two kinds of paths have similar t* values, since all paths are in the high Q lithosphere. In the range $10° < \Delta < 20°$ the t* values diverge, the raypaths under the WUS penetrate the low Q, low velocity layer and they become severely attenuated. At greater epicentral distances the t* values most likely remain constant, the difference between the two populations in t* is roughly constant, and is caused by the difference in attenuation along the WUS leg of the wavepaths. The minimum t* difference $\Delta t^*_{min} = .18$ needed to explain a regional body wave magnitude variation of .25 is also indicated in the figure. Although some points in the two populations are closer than that, the differences in the <u>mean t* values</u> over greater distance ranges, as shown above, are sufficient to explain the magnitude anomalies.

The t* value .75 of Helmberger (1973) used for computing synthetic seismics in the distance range indicated is somewhat higher than our values, while

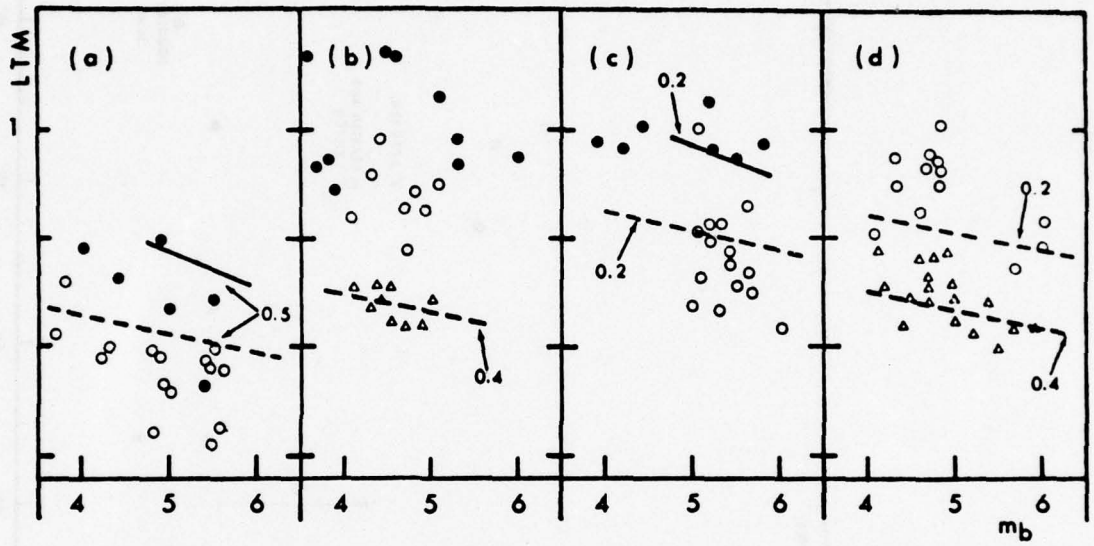

Figure 6a. LTM discrimants at NORSAR for events located in various regions of the world (after Noponen,1975). Explosion and earthquake observations are plotted with filled and open symbols, respectively. (a) Events in southwestern North America. (b) Explosions in western Russia, earthquakes in southern Greece (circles) and Turkey (triangles). (c) Events in Central Asia. (d) Earthquakes at Kuriles (circles) and Sakhalin (triangles). Almost all of the events in the figure are shallow, and none is deeper than 100 km. Lines denote LTM theoretical values computed for t* values indicated in the figure for explosions (solid lines) and earthquakes (dash lines).

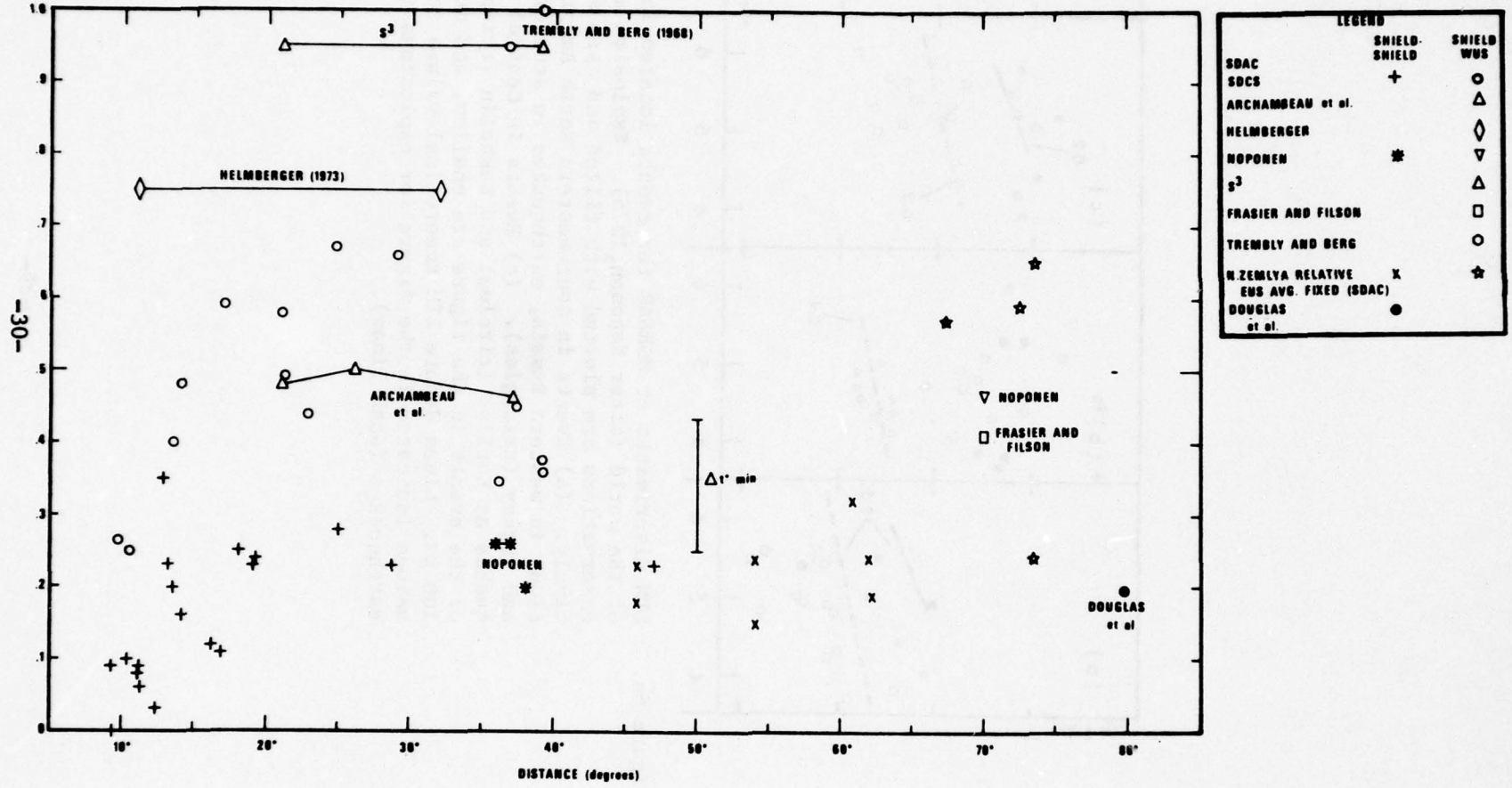

Figure 6b. Summary of all t* data in Table I as functions of epicentral distance.

those derived from the velocity and Q model of Archambeau, et al. (1969) seem, on the average, to be on the low side. The lowest value used by Bache, et al. (1976) t* = .95 (they used values as high as 1.15), one point of ours and the value of Trembly and Berg (1968) seem to be extremely high relative to the rest of the values.

Losses in shear deformation would also imply that spectral differences should be even greater for short-period S-waves. There are no t* determinations for short-period S over teleseismic distances in North America. Statistical analysis of short-period S amplitudes and dominant periods, however, showed that the short-period S-waves have significantly lower amplitudes and longer dominant periods in the WUS (Der, Massé, and Gurski, 1975). Figure 7 shows a map of LRSM stations classified with respect to S-wave attenuation into three groups (high, intermediate and low attenuation) by a statistical procedure. The region of high attenuation coincides with the region of negative magnitude residuals of Booth, Marshall and Young (1974). Since the dominant frequency of S-waves is lower (.5 Hz) in the EUS, the amplitude effect on short-period S-waves is not as great. Figure 8a shows the distribution of periods of short period S waves in the two parts of the country. The data from the deep focus events in Der, Massé, and Gurski (1975) were used to construct this figure. The mean period of S-wave for each event $\frac{1}{2}(T_{EUS}^{av} + T_{WUS}^{av})$, where T_{EUS}^{av} and T_{WUS}^{av} are the averages of dominant periods of short-period S-waves in the EUS and the WUS respectively, was subtracted from each measured value prior to plotting a histogram. The histogram show that the S-wave periods are on the average 1 second longer in the WUS, indicating a significant spectral difference. The regional correlation between short-period P and S-wave attenuation in consistent with the hypothesis that the cause of regional bias is anelastic attenuation and that a considerable part of the losses occurs in shear deformation.

Bache, T. C., T. G. Barker, N. Rimer and J. M. Savino, 1976, Comparison of theoretical and observed body and surface waves for Kasseri, an explosion at NTS, Systems, Science and Software, SSS-R-76-2937.

Trembly, L. A., and J. W. Berg, 1968, Seismic source characteristics from explosion-generated P-waves, Bull. Seism. Soc. Am., v. 58, p. 1833-1848.

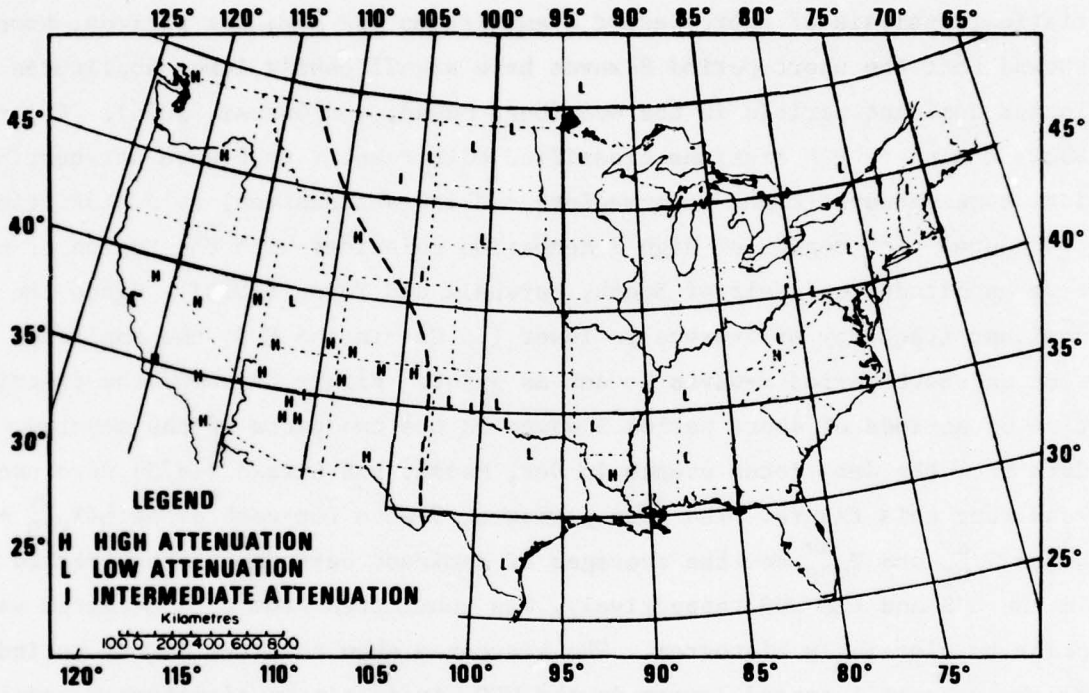

Figure 7. Map of short-period S-wave attenuation after Der, Massé and Gurski (1975).

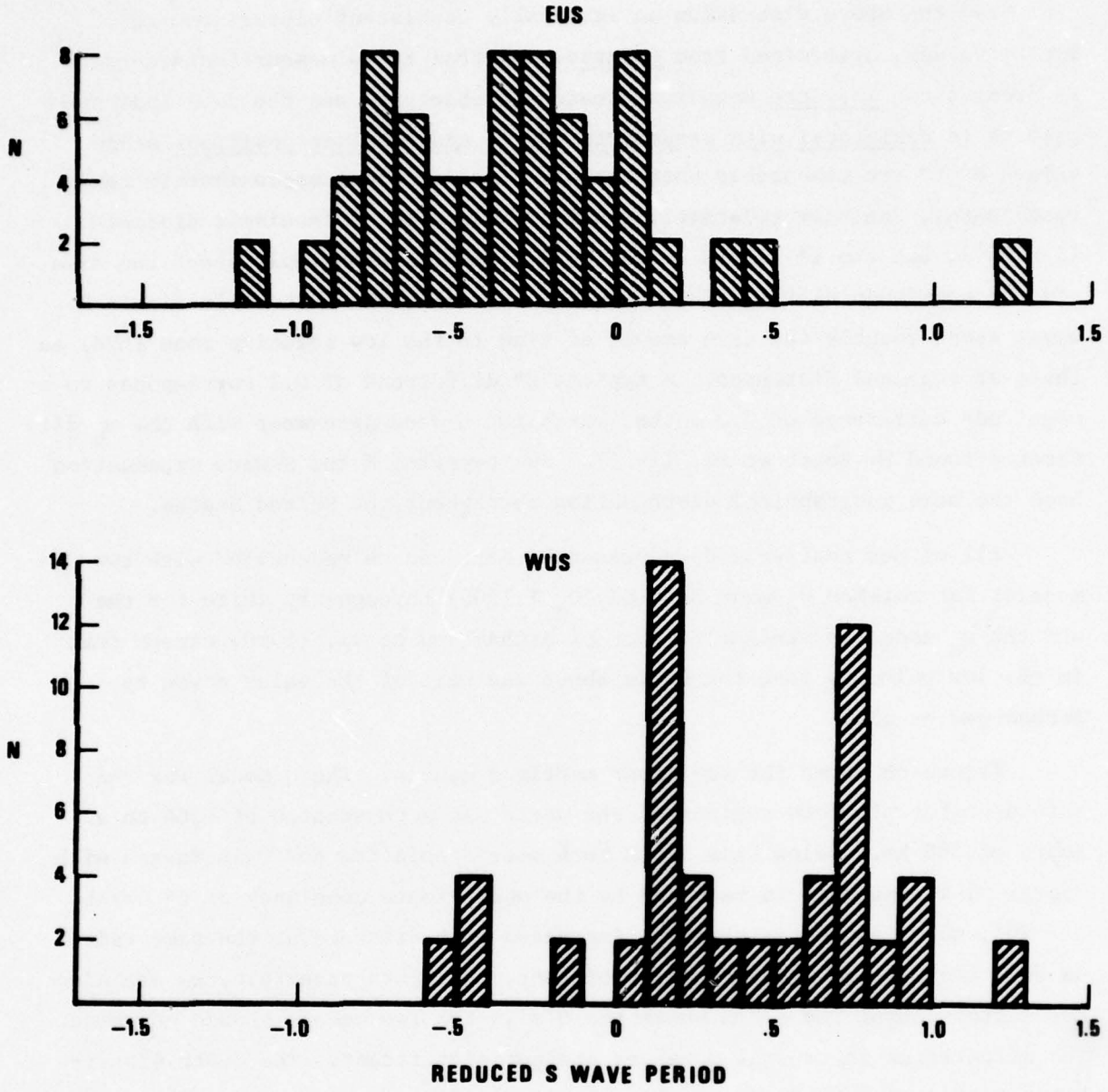

Figure 8a. The distribution of S-wave periods in the WUS and EUS. (Average of periods for each event is subtracted).

From the above discussion an internally consistent picture emerges. The t* values, determined from relative spectral ratio measurements correctly predict the absolute magnitude residuals observed, and the data indicate that t* is reciprocal with respect to source and receiver positions since values of t* are comparable when the waves travel along approximately reciprocal paths. We have relatively fewer t* values for teleseismic distance ($\Delta > 35°$), but the t* values at regional distances also imply about the same size of magnitude differential which is reasonable since the teleseismic P-waves spend roughly the same amount of time in the low velocity zone (LVZ) as those at regional distances. A typical t* difference of 0.2 corresponds to a magnitude difference of 0.3 units, which is in good agreement with the m_b difference found by Booth et al. (1975). Short-period P and S-wave attenuation have the same geographical distribution throughout the United States.

All of our available data presented here can be reconciled with two Q_α models; for shields Q_α must be high ($Q_\alpha \gtrsim 1500$) throughout, while for the WUS the Q_α model is similar to that of Archambeau et al. (1969) except that in the low velocity zone the Q_α is about one half of the value given by Archambeau et al.

Figure 8b shows the two upper mantle Q models. The Q model for the shield/stable platform regions of the world has a constant Q of 1500 to a depth of 400 km. Below this depth both models coincide and Q increases with depth. This increase is required by the approximate constancy of t* beyond $\Delta > 20°$, which indicates that Q_{av} increases with distance at the same rate as does travel time. Fine details of both models are uncertain, we are also not certain about the depth where the Q's in the two models should converge. The differences in crustal Q values are not significant. The depth distributions of Q given here are qualitatively similar to those for Q_β by Lee and Solomon (1975) who derived their model from surface-wave attenuation.

Lee, W. B., and S. C. Solomon, 1975, Inversion schemes for surface wave attenuation and Q in the crust and the mantle, Geophys. J. R. Astr. Soc., v. 43, p. 47-71.

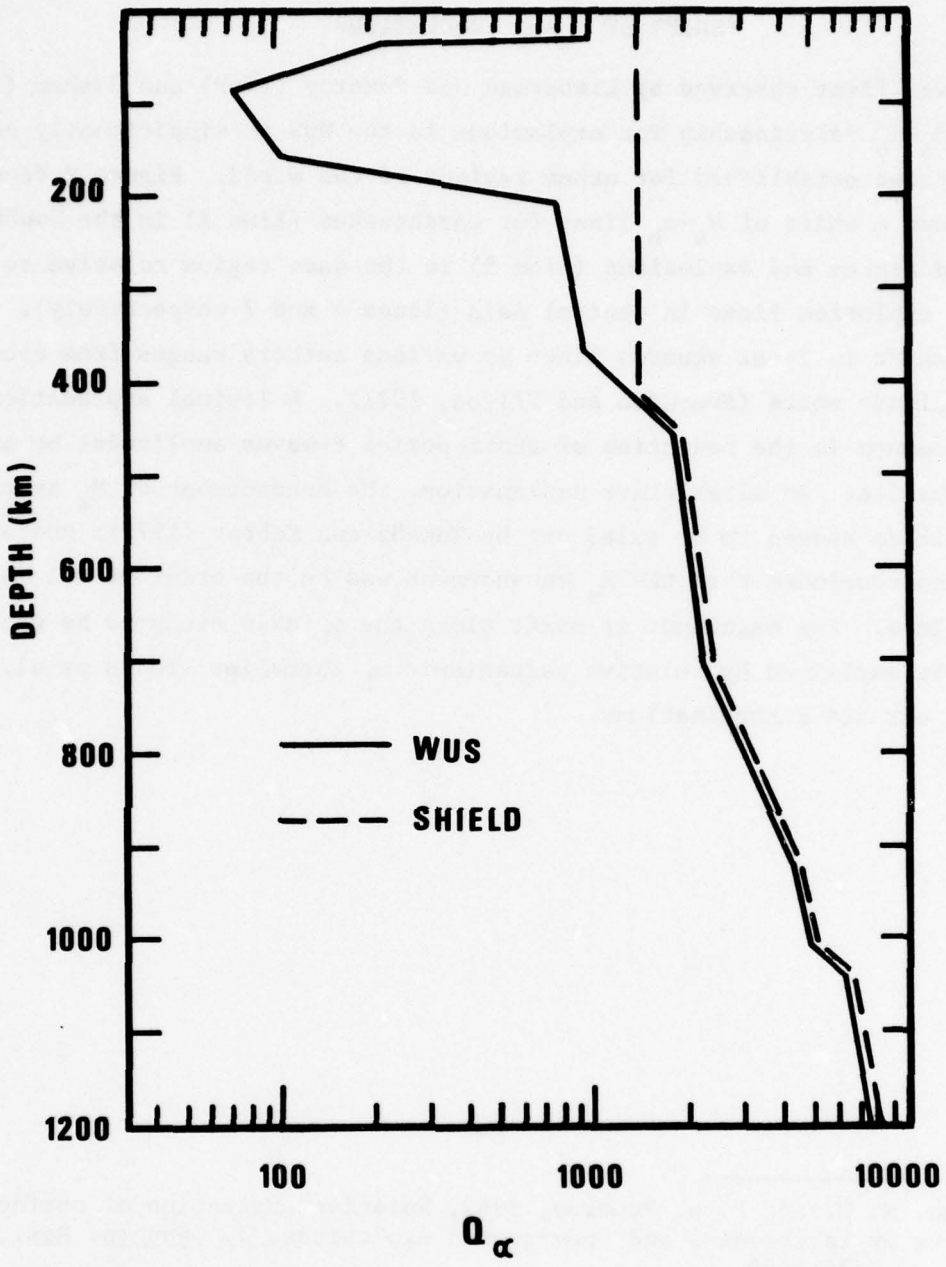

Figure 8b Two Q models for short-period P-waves which satisfy the data presented in this report.

SHIFT OF M_s-m_b POPULATIONS

It was first observed by Lieberman and Pomeroy (1969) and Basham (1969) that the M_s-m_b relationship for explosions in the WUS is significantly different from those established for other regions of the world. Figure 9 from Basham shows a shift of M_s-m_b lines for earthquakes (line 1) in the Southwestern United States and explosions (line 5) in the same region relative to earthquake and explosion lines in Central Asia (lines 4 and 7 respectively). The relative shift in least squares lines by various authors ranges from about .3 to .5 magnitude units (Evernden and Filson, 1971). A logical explanation for this phenomenon is the reduction of short-period P-waves amplitudes by anelastic attenuation. An alternative explanation, the enhancement of M_s by tectonic stress release seemed to be ruled out by Toksöz and Kehrer (1972); and by Masse (1973), who concluded that the M_s enhancement was on the order of 0.1 magnitude units or less. The magnitude of shift along the m_b axis seems to be greater than can be explained by relative teleseismic m_b anomalies (Booth et al., 1975) and our Δt^* determinations.

Liebermann, R. C. and P. W. Pomeroy, 1969, Relative excitation of surface waves by earthquakes and underground explosions, J. Geophys. Res., v. 74, p. 1575-1590.

Basham, P. W., 1969, Canadian magnitudes of earthquakes and nuclear explosions in Southwestern North America, Geophys. J. R. Astr. Soc., v. 17, p. 1-13.

Evernden, J. and J. Filson, 1971, Regional dependence of surface-wave versus body-wave magnitude, J. Geophys. Res., v. 76, p. 3303-3308.

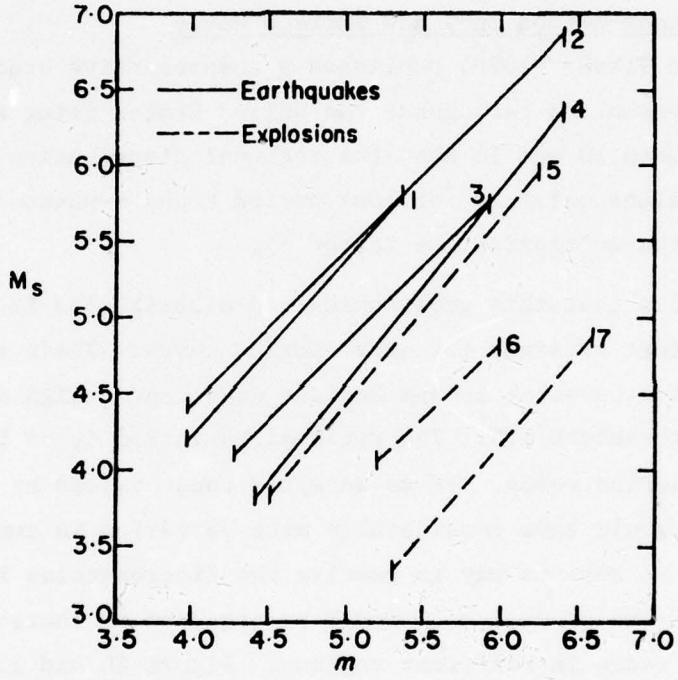

Figure 9. M_S-m_b relationships for earthquakes and explosions in various regions of the world (after Basham 1969).

SUPPORTING EVIDENCE FOR HIGH ATTENUATION UNDER THE WUS

General

In this section we present evidence supporting the notion of a highly attenuating, parially molten upper mantle under the WUS. Some of the evidence is directly related to short-period attenuation (attenuation at long periods) and some is indirectly related. Special attention will be given to similarities in the geographical distributions of various geophysical variables.

Attenuation of Long-Period Body and Surface Waves

Solomon and Toksöz (1970) published a comprehensive study of long-period P and S-wave attenuation throughout the United States using the spectral ratio method. Figures 10 and 11 show the regional distribution pattern of relative t* (δt^*) values obtained for long period P and S-waves (their definition of t* includes the multiplicative factor π).

It is obvious that this geographical t* distribution is significantly different from that obtained for short-period waves. Their map shows a low attenuation region parallel to the Pacific Coast and a high attenuation region in the northeastern U.S. The regional variation in t* is also greater than for short-period waves. If we accepted these values as δt^* for short-period waves we would have considerably more variation in amplitudes than that observed. An obvious way to resolve the discrepancies is to propose the frequency dependence of Q, i.e. Q would be required to increase with frequency at different rates in different regions. Figure 10 and 11 are based on data from two deep Peru-Brazil border events which also may have led to discrepancies due to radiation pattern effects. It is important, however, that the area of prime interest in our study, the Basin and Range province is characterized by high attenuation for both long-period P and S-waves. The values of δt^* for P and S seem to be related by the 4:1 relationship proper for losses entirely in shear (Figure 12).

Theoretical studies of a solid matrix with viscous liquid inclusions of large aspect ratios show that such media attenuate the seismic waves passing

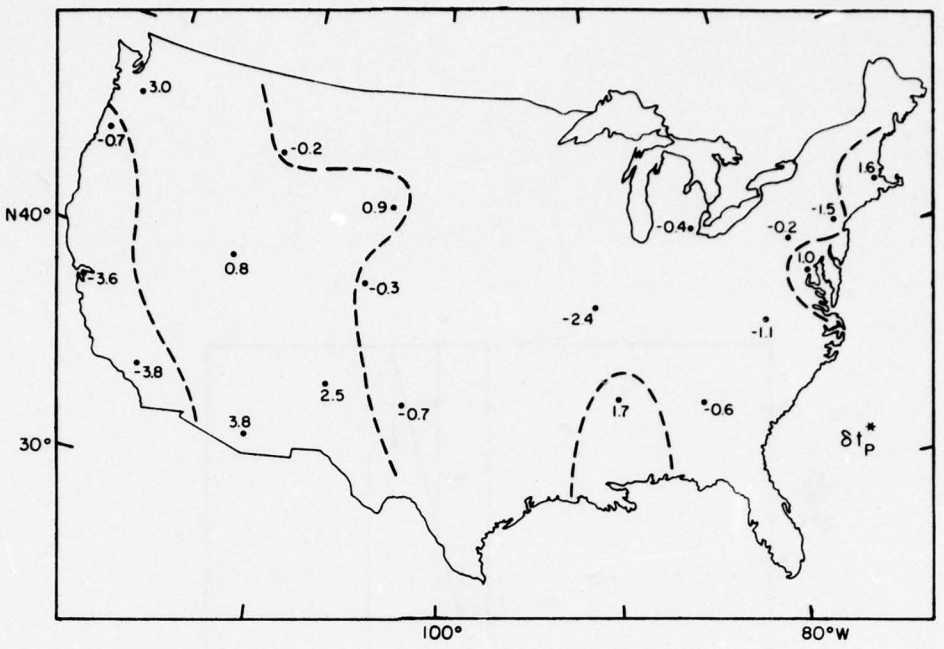

Figure 10. t* values for long-period P-waves in the United States (after Solomon and Toksöz 1970).

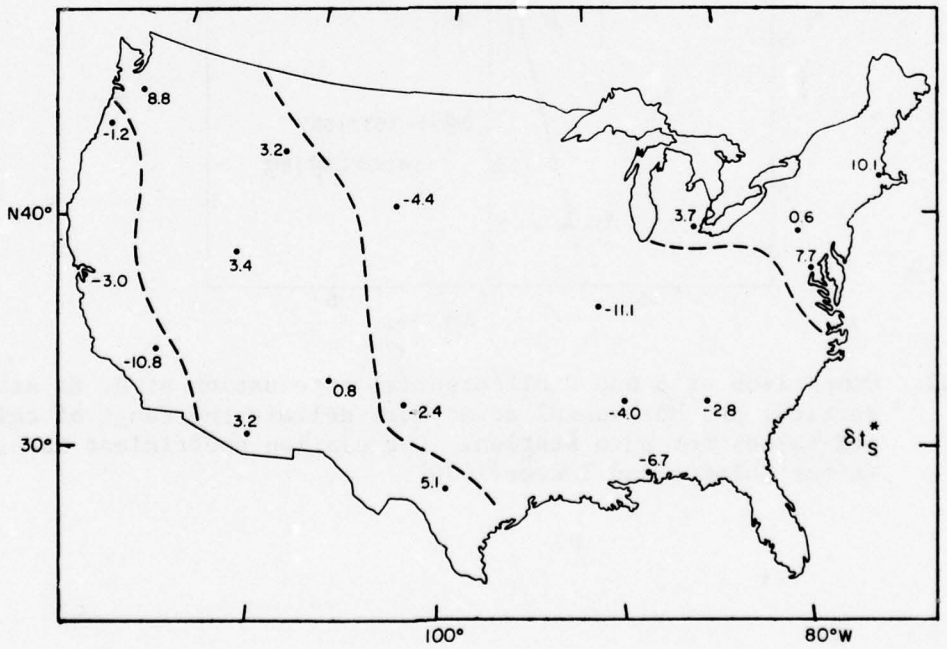

Figure 11. t* values for long-period S-waves in the United States (after Solomon and Toksöz 1970).

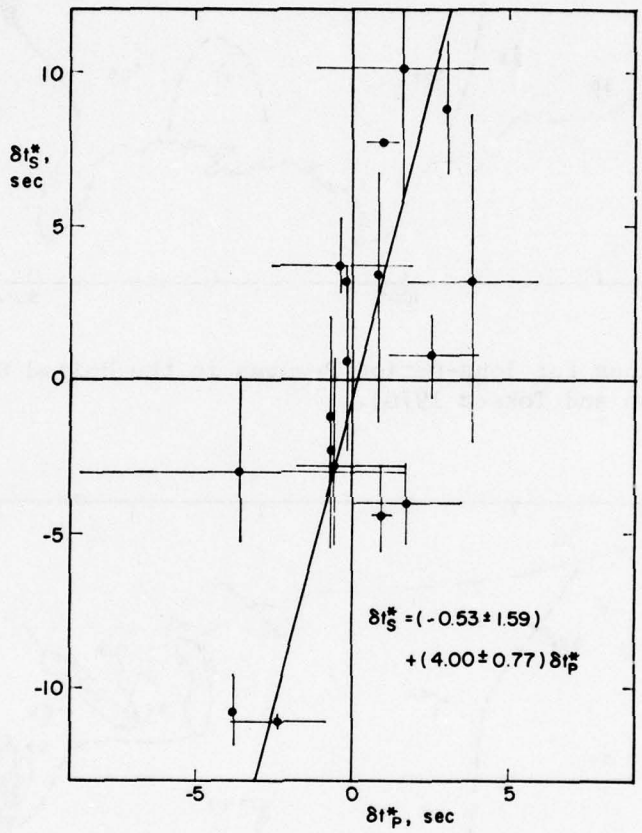

Figure 12. Comparison of S and P differential attenuation at U. S. stations. Vertical and horizontal error bars delimit the range of calculated values for each station. Correlation coefficient is 0.67 (after Solomon and Toksöz 1970).

through them (Walsh 1968, 1969). The attenuation is, in general, frequency dependent: the form of this dependence and the amount of attenuation is determined by the aspect ratios, the properties of the solid matrix, the concentration and viscosity of liquid inclusions. This model also requires that all of the attenuation occurs in shear deformation, and none in compression. This seems to be a realistic model for a partially molten rock where some mineral components are solid while others have melted, and the shape of inclutions, naturally, cannot be expected to be equidimensional. A solid matrix with inclusions of various concentrations and shapes can explain a wide range of frequency-attenuation relationships. The model implies that neither the regional distribution nor the degree of attenuation (Q) must be related at different frequencies if the model changes laterally. Such laterally changing models can explain the differences in the regional distribution patterns obtained at different frequencies. It is significant, however, that the attenuation is higher in the WUS for both short and long-period waves. The solid matrix with liquid inclusions also has wave velocities lower than that of the homogeneous solid with the properties of the matrix. Besides, dispersion due to attenuation may make the delays dependent on the frequency of waves. This model, therefore, also explains the travel time delays without assuming compositional changes. The sole requirement is that the temperatures become high enough to melt some mineral components of the rock.

Solomon (1972) attempted to model the observed attenuation and travel time delays by the superposition of two attenuation mechanisms. Although his model is plausible, it is not unique since too many parameters are not surficiently known. Nevertheless, detailed studies of the frequency and regional dependence of attenuation and travel time, as well as other data, may eventually make it possible to build a more unique geophysical model of the Western United States.

Walsh, J. B., 1968, Attenuation in partially melted material, J. Geophys. Res., v. 73. p. 2209-2216.

Walsh, J. B., 1969, New analysis of attenuation in partially melted rock, J. Geophys. Res., v. 74, p. 4333-4337.

Solomon, D. C., 1972, Seismic-wave attenuation and partial melting in the upper mantle of North America, J. Geophys. Res., v. 77, p. 1483-1502.

Studies of long-period surface wave attenuation across the WUS and the EUS (Lee and Solomon 1975) also indicate a low Q layer coincident with the low velocity layer under the Western United States, while such a layer is absent in the EUS. Figure 13 shows their values of $100/Q_\beta$ plotted for various regions of the United States, indicating such a layer (high $100/Q_\beta$ values) under the WUS.

Travel Time Delays

It has also been observed that the travel times of body waves to the WUS are consistently late (Cleary and Hales, 1966; Doyle and Hales, 1967; Hale and Roberts, 1970). Travel times are not related directly to attenuation since compositional variations can also cause changes in travel times although, as stated above, the physical model of partial melting of identical rocks can explain such changes without the need for assuming compositional changes. Figure 14 shows P-wave travel time residuals from deep events obtained by Julian and Sengupta (1973). These correlate well with the geographical distribution of magnitude residuals according to Booth et al. and the attenuation maps of Der et al. The same correlation is evident on the map of S-wave residuals by Doyle and Hales (1967) (Figure 15) and Hales and Roberts (1970) (Figure 16); the values shown were derived from both deep and shallow events and thus may be contaminated with near source travel time effects. The picture is fairly consistent, however, showing late arrivals in the WUS and early arrivals in the EUS. Except for some mixed delay values in California there is no correlation with the coastal strip of low long-period attenuation reported by

---

Cleary, J., and A. L. Hales, 1966, An analysis of the travel times of P-waves to North American stations, in the distance range 32° to 100°, Bull. Seism. Soc. Am., v. 56, p. 467-489.

Doyle, H. A., and A. L. Hales, 1967, An analysis of the travel times of S-waves to North American Stations in the distance range 28° to 82°, Bull. Seism. Soc. Am., v. 57, p. 761-771

Hales, A. L., and J. Roberts, 1970, The travel times of S and SKS, Bull. Seism. Soc. Am., v. 60, p. 461-489.

Julian, B. R., and M. Sengupta, 1973, Travel time anomalies for the global station network, Semiannual Technical Summary, Seismic Discrimination, ESD-TR-73-348, Lincoln Laboratories, MIT, Lexington, Massachusetts.

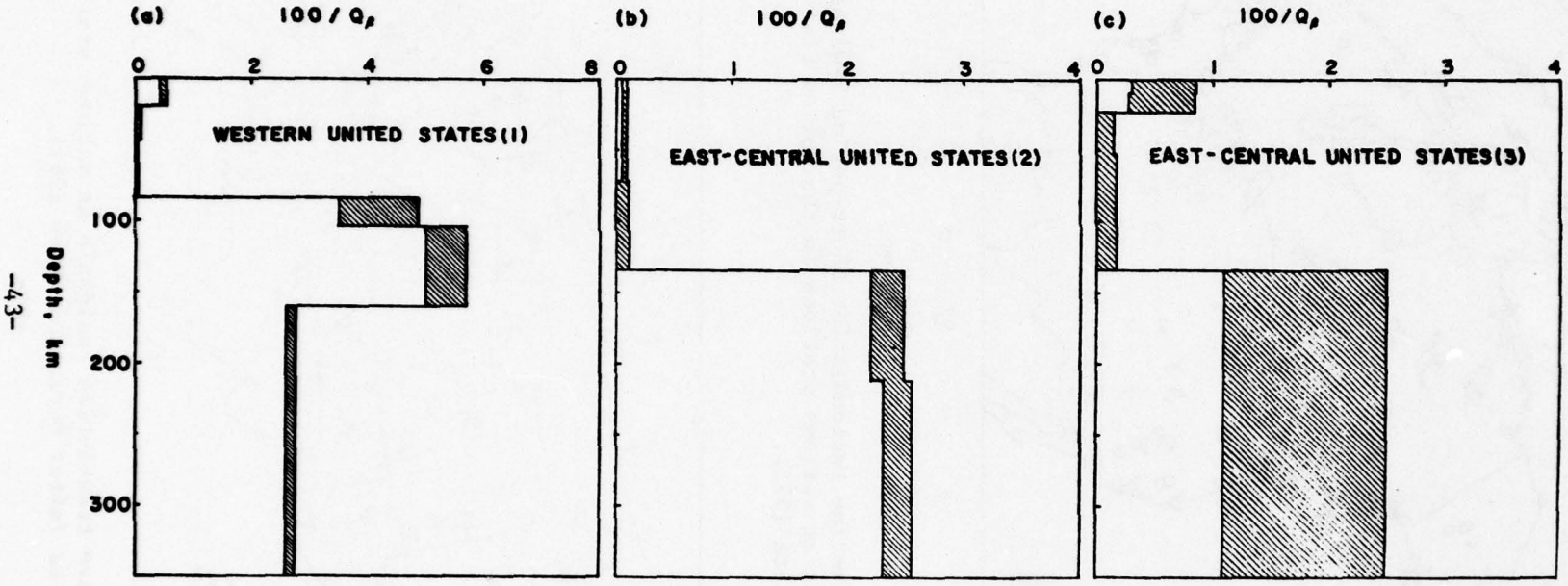

Figure 13. Limits of $100/Q_\beta$ regions of the United States (after Lee and Solomon 1975).

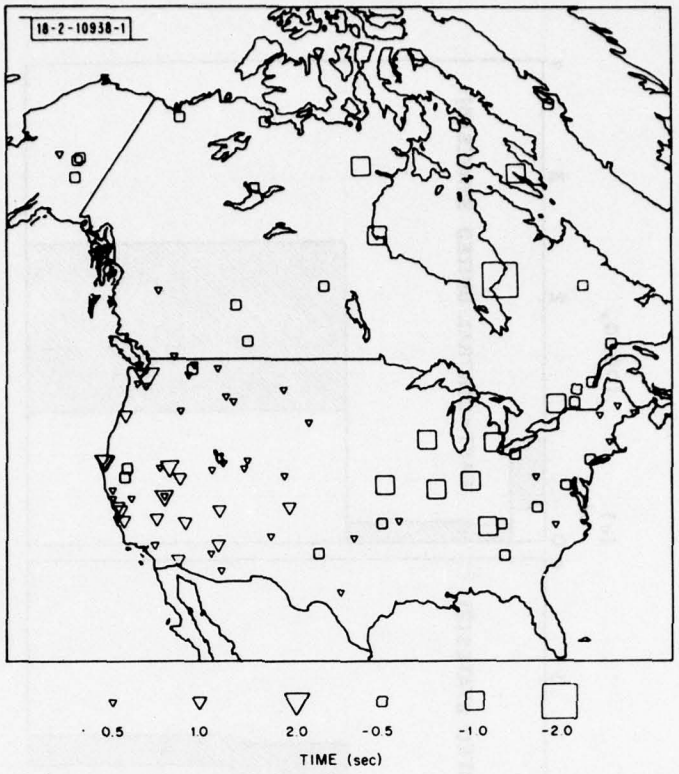

Figure 14. Travel-time residuals for short-period P-waves from deep earthquakes at various stations in the United States (after Julian and Sengupta 1973).

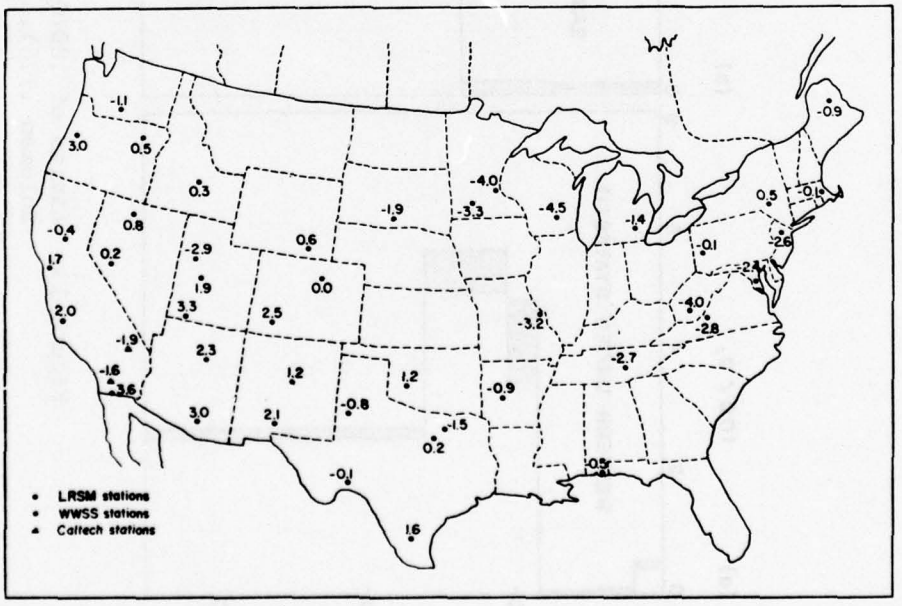

Figure 15. S-wave travel-time residuals at various stations in the United States (after Doyle and Hales 1967).

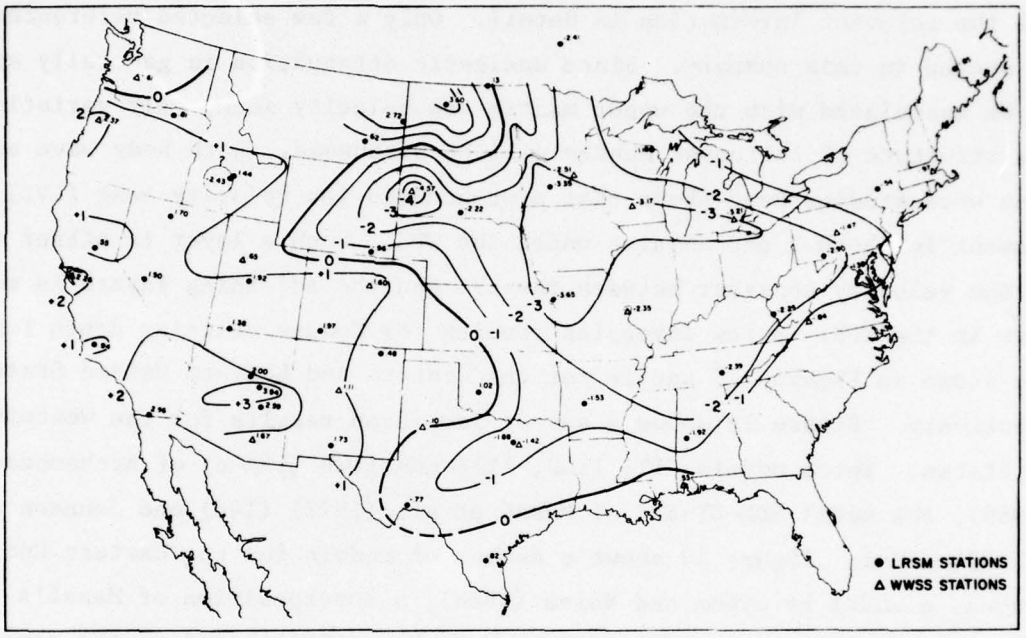

Figure 16. S and SKS travel-time residuals in the United States (after Hales and Roberts 1970).

Solomon and Toksöz (1970) nor with their high attenuation region in the Northeastern United States. Comparison of the magnitude of P and S-wave travel time delays shows that the S-wave delays are about four times greater than the P-wave delays. This is consistent with the notion of complex shear modulus caused by partial melting under the Western United States.

Velocity Structure

The crust-upper mantle structure under the United States is widely discussed in the literature. It is beyond the scope of this report to discuss all the relevant information in detail. Only a few selected references will be quoted in this summary. Since anelastic attenuation is generally assumed to be associated with the upper mantle low velocity zone, only variations in the structure of the upper mantle will be discussed. Both body wave and surface wave studies have shown that a pronounced low velocity zone (LVZ) is present for both P and S-waves under the WUS. Such a layer is either absent or the velocity contrast between the LVZ and the adjoining layers is much less in the EUS. A few inversion results for P-wave velocity depth function are shown in Figures 17 and 18 for the Western and Eastern United States respectively. Figure 18 shows a set of inversion results for the Western United States. Three models CIT, 110P, 111P and 112P (14a-c) of Archambeau et al. (1969), the model SDL-UT-BR1 of Massé et al. (1972) (14d) and Johnson's model CIT 204 model. Figure 19 shows a number of models for the Eastern United States, a model by Green and Hales (1968), a superposition of Massé's (1973) EUS model (MAS) with a model VIC3 by McMechan (1975) based on the same data; and the model YULKNFIO by Julian (1970).

Massé, R. P., M. Landisman, and J. B. Jenkins, (1972), An investigation of the upper mantle compressional velocity distribution beneath and Basin and Range Province. Geophys. J. R. Astr. Soc., v. 30, p. 19-36.

Green, R. W. E., and A. L. Hales, 1968, The travel times of P-waves to 30° in the central United States and upper mantle structure, Bull. Seism. Soc. Am., v. 58, p. 267-290.

McMechan, G. A., 1975, Amplitude constraints and the inversion of Canadian Shield Early Rise Explosion data, Bull. Seism. Soc. Am., v. 65, p. 1419-1433.

Julian, B. R., 1970, Regional variations of upper mantle structure beneath North America, Ph.D. Thesis, California Institute of Technology.

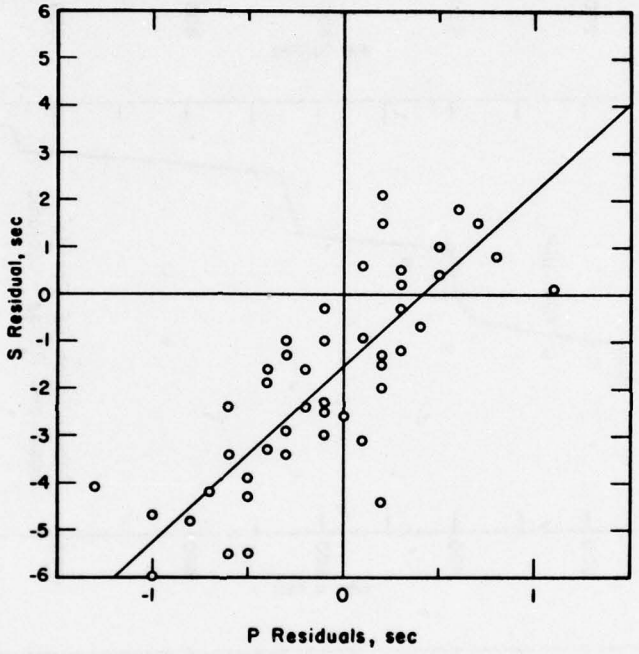

Figure 17. P and S-wave travel-time delays indicating a linear correlation (Doyle and Hales 1976).

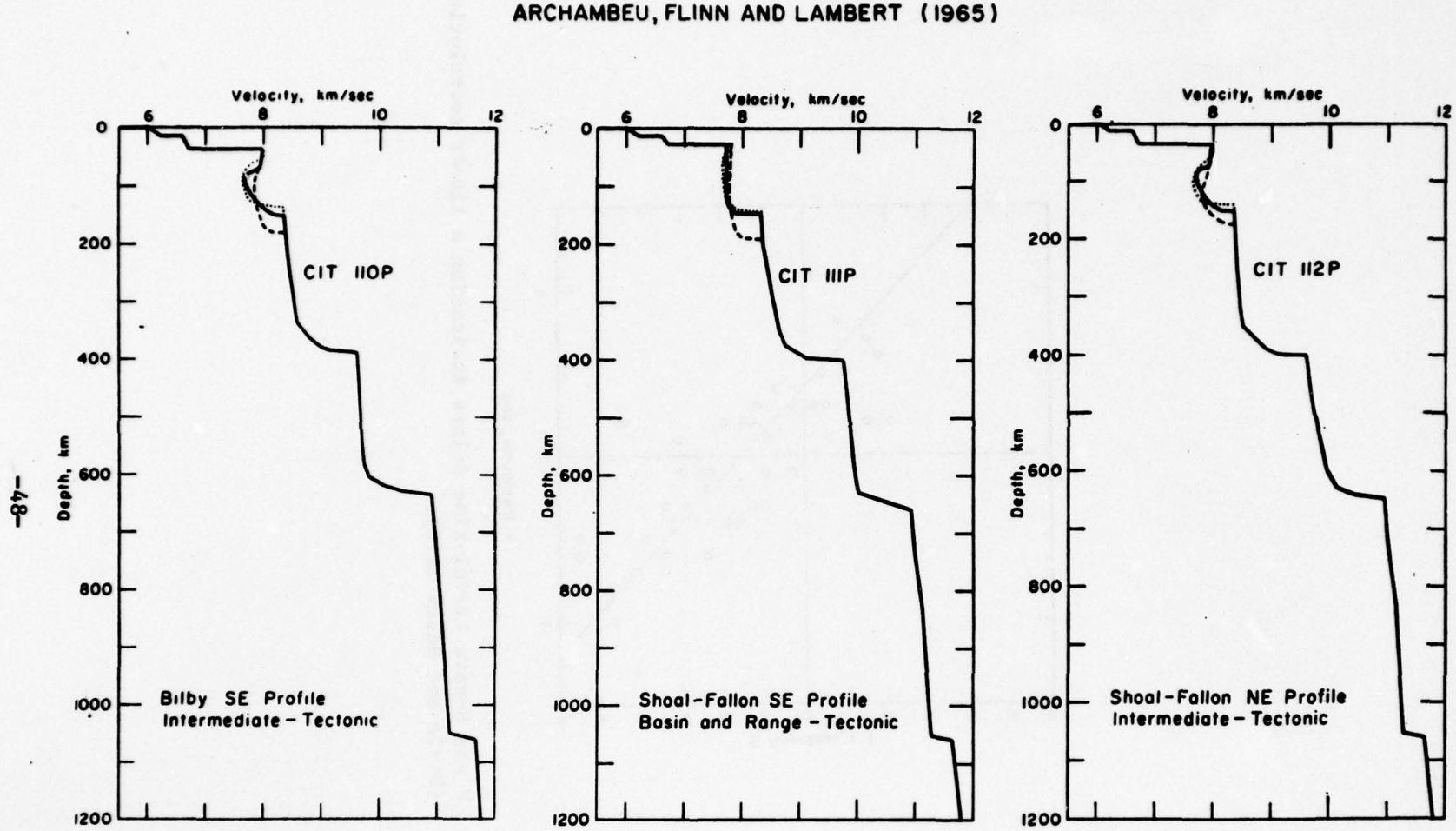

Figure 18. Selected P-wave velocity models for the Western United States.

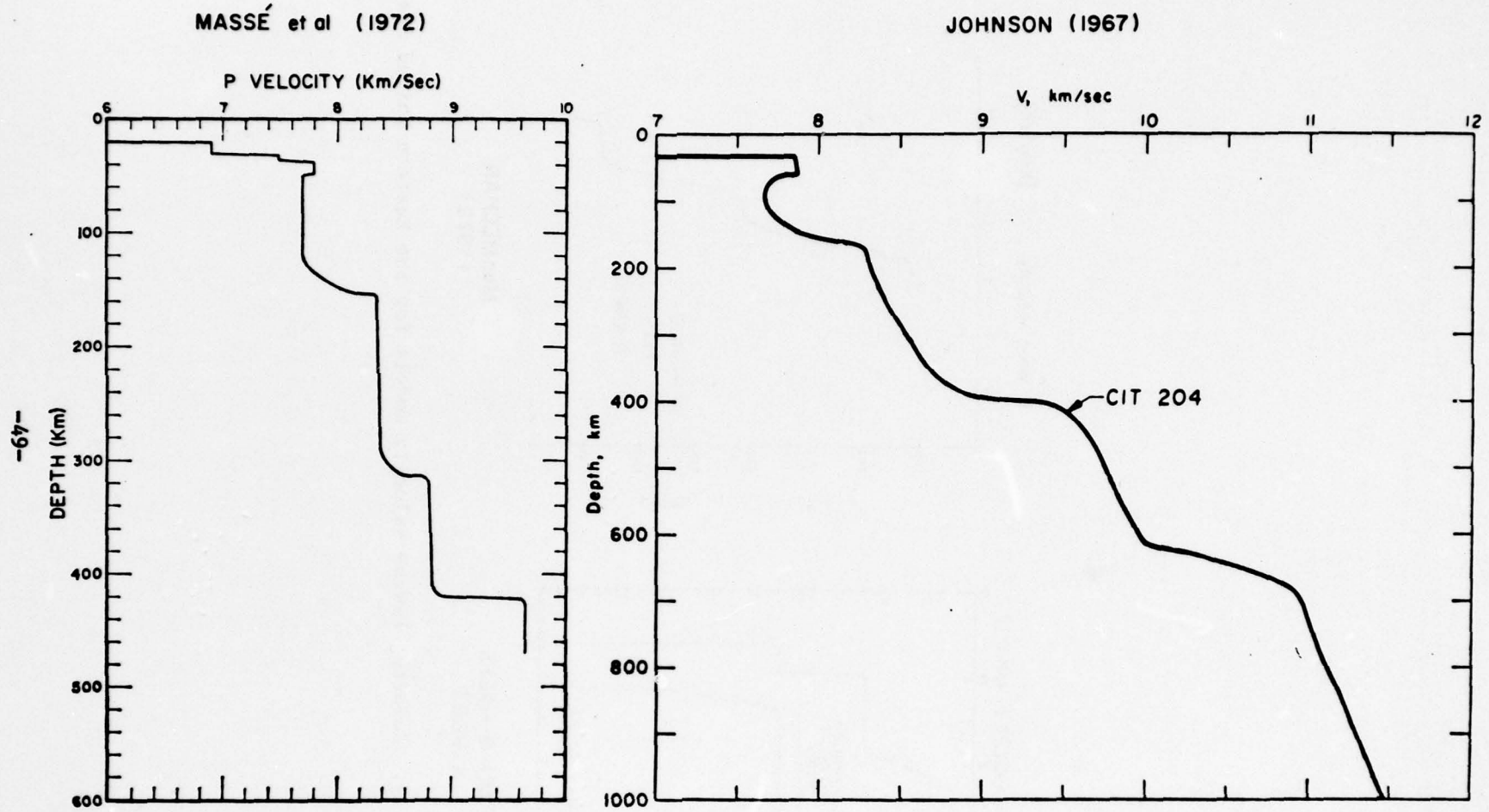

Figure 18. (Continued) Selected P-wave velocity models for the Western United States

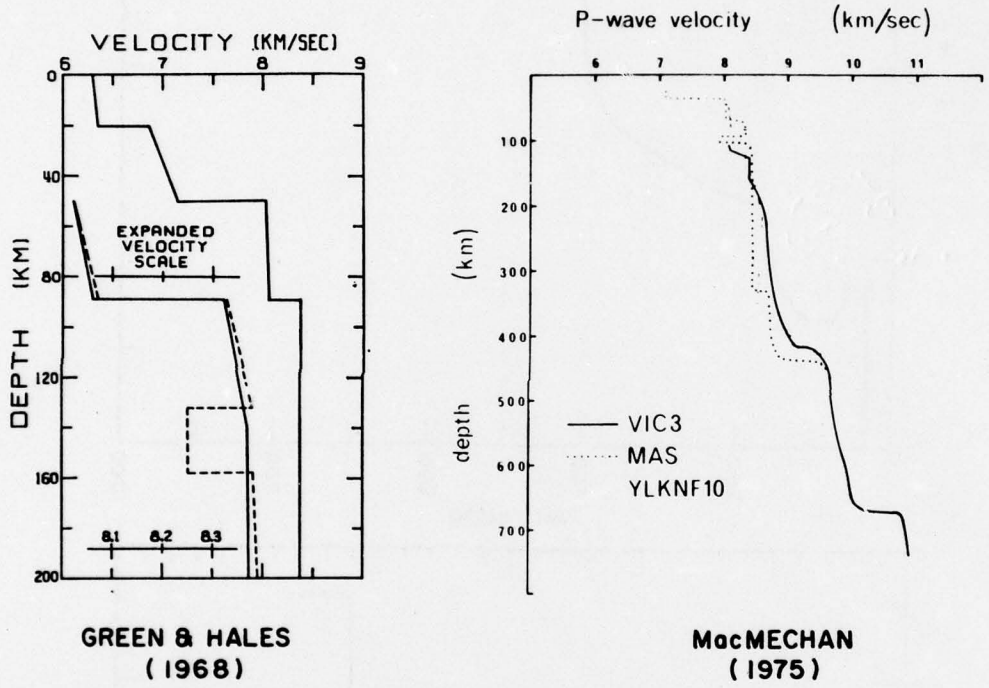

Figure 19. Selected P-wave velocity models for the Eastern United States.

We exclude three models from our presentation: the Wiggins and Helmberger (1973) models HWA and HWB, which were derived by using data from a few close-in stations. The definition of these models at the depth of the LVZ is poor (the authors state this themselves); the model HWNE by the same authors is excluded for the same reason. These models are more relevant to deeper mantle structure, the 450 and 700 km velocity gradient regions, that we are not particularly concerned with in this summary.

Inspecting the rest of the selected models it becomes obvious that the crust-upper mantle structure is quite different in the two major subdivisions of the continent. The WUS is underlain by an upper mantle low-velocity layer. In most inversions one finds a "lid" of higher velocity just under the Mohorovicic discontinuity. In some places the lid may be missing and the low-velocity region reaches the base of the crust (see Model CIT 111P) resulting in extremely low P_n velocities. In the EUS the low velocity layer is missing (disregarding an insignificant velocity inversion) the velocities remain above 8 km/sec and increase with depth everywhere below the Mohorovicic discontinuity. The P_n (sub-Moho) velocities are above 8 km/sec everywhere in the EUS as shown by a map of Herrin and Taggart (1962) which is reproduced in Figure 20. The high P_n velocity regions in the WUS do not necessarily mean the absence of LVZ or attenuation in those regions, rather, they reflect the variations in the "lid" zone. A fairly good correlation between P_n velocity and station residuals exists, however, since low (<8 km/sec) P_n velocities occur only in the WUS. The WUS is also characterized by high S_n attenuation (Molnar and Oliver 1969).

Many authors have derived the velocity structure for S-waves. The most recent comprehensive study of the subject was done by Biswas and Knopoff (1974). They found a sizeable S-wave low-velocity layer under the WUS. The same layer is either absent or much reduced in size in the EUS. The exis-

---

Herrin, E., and J. Taggart, 1962, Regional variations in P_n velocity and their effect on the location of epicenters, Bull. Seism. Soc. Am., v. 52, p. 1037-1046.

Biswas, N. N., and L. Knopoff, 1974, The structure of the upper mantle under the United States for dispersion of Rayleigh waves, Geophys. J. R. Astr. Soc., v. 36, p. 515-540.

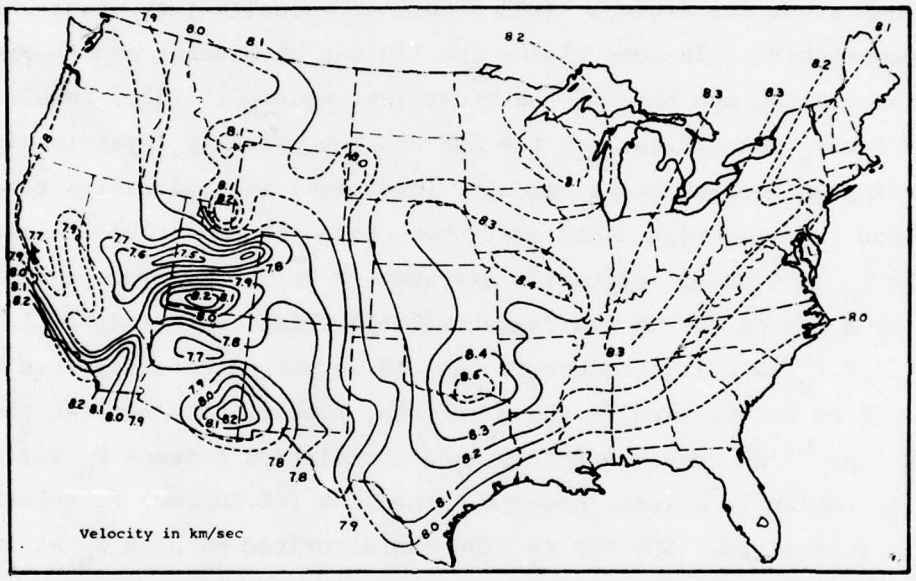

Figure 20. P_n velocity under the United States. (Herrin and Taggart 1962).

tence of P and S-wave low-velocity layers is also consistent with the partial melting model described above, since melting would reduce both the wave velocities in the material, but the reduction of S-wave velocity would be greater. This is in agreement with the observation that the low-velocity layer is more pronounced for S-waves, but if a prominent S-wave low-velocity layer is present there is one for P-waves also.

Upper Mantle Resistivity and Heat Flow

Analysis of magnetic variations in the WUS has revealed wide-spread conductive regions in the upper mantle. Figure 21, a map from Gough (1973) shows the areal distribution of the conductive regions (the density of stippling is proportional to conductivity). The correlation with short-period amplitude anomalies is only fair; here we have a coastal strip of low conductivity and the Wyoming Basin-Colorado Plateau stand out as regions of low conductivity. The Basin and Range province shows high conductivity. The highest conductivities are found in the Rocky Mountain frontal regions and a long strip in Western Utah. Gough estimates that the conducting layer is between 50 and 100 km depth in the upper mantle, but interpretation of such anomalies is not unique. Vertical topography of the top of the conductive region also influences the values of the conductivity measured. In areas of low apparent conductivity the conductive layer may still be present at a greater depth. Correlation of these anomalous conductivities with heat flow data is fairly good (Sass et al. 1971), as shown in Figure 22. The heat flow measurements can be influenced by many factors, such as groundwater circulation, sedimentary thicknesses, etc., and as a result may not be consistent indicators of conditions in the upper mantle.

Laboratory studies of rocks indicate that the resistivity of rocks decreases by several orders of magnitude as the rock starts to melt. An increase in temperature of course will also lead to increased heat flow.

Gough, D. I., 1973, The geophysical significance of geomagnetic variation anomalies, Phys. Earth. Planet. Int., v. 7, p. 379-388.

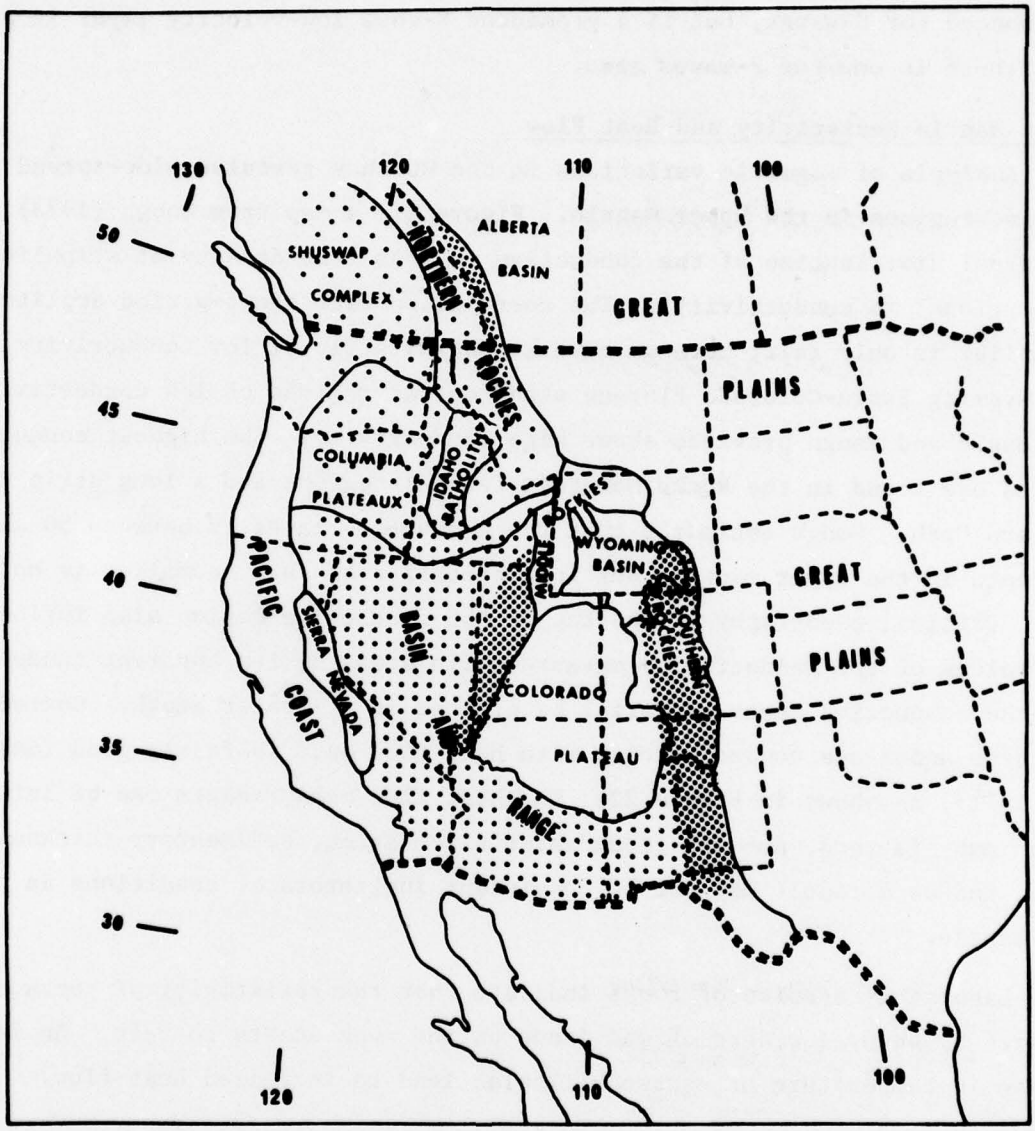

Figure 21. Upper mantle conductivity map. Density of stippling proportional to conductivity. (Gough 1973).

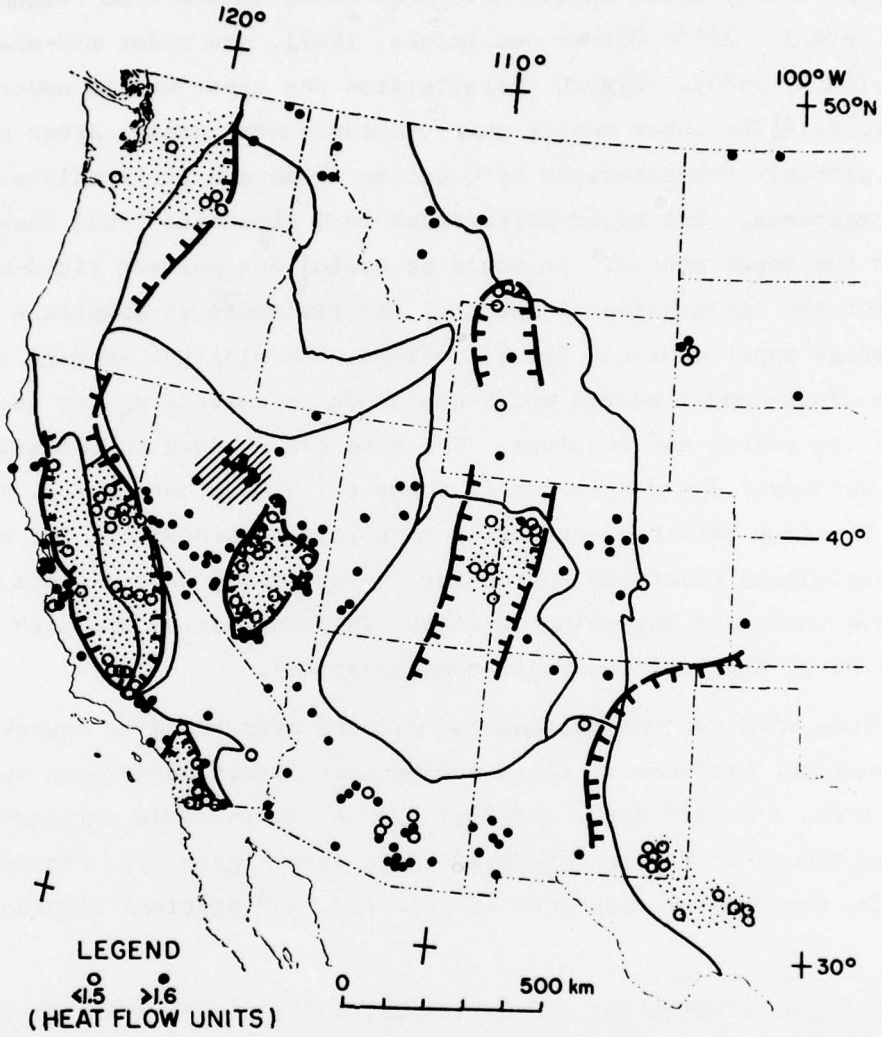

Figure 22. Heat flow measurements in the Western United States.

GENERAL COMMENTS

Most of the discussion in this report has centered on the relative t* differences along paths in the United States. Major differences in Q structure have been found, however, in many other areas of the world. Extremely low-Q regions in the upper mantle have been found behind some island arcs (Barazangi et al., 1975; Oliver and Isacks, 1967), and under mid-oceanic ridges (Solomon, 1973). High-Q characterizes the upper mantle under continental shields. The upper mantle under tectonic continental areas and average oceans is probably characterized by Q values which are intermediate between these two extremes. The major differences in Q structure found thus far are located in the upper mantle. It would be useful for correct yield-m_b estimation and for the application of spectral discriminants to compile a worldwide map of average upper mantle Q (or t*) values. Knowing the average attenuation properties of the upper mantle would enable us to correct m_b for attenuation under both the source and receiver. The same can be done to teleseismic body-wave spectra. The deeper mantle seems to be more homogeneous laterally in Q, and it seems that two correction factors are needed; one for attenuation in the upper mantle under the source for the downgoing wave and one for the upgoing wave under the receiving station. This suggestion was also made earlier by P. D. Marshall (personal communication).

Magnitude bias in some regions can also be attributed to causes other than attenuation. Presence of thick sedimentary layers under some regions (stations along the Gulf Coast and Florida) is the probable explanation of the high amplitude of P-waves observed there (see Figure 1). Preliminary calculations for crustal responses at selected LRSM stations located both in

---

Barazangi, M., W. Pennington, and B. Isacks, 1975, Global study of seismic wave attenuation in the upper mantle behind island arcs using pP-waves J. Geophys. Res., v. 80, p. 1079-1092.

Oliver, J., and B. Isacks, 1967, Deep earthquake zones, anomalous structures in the upper mantle and the litosphere, J. Geophys, Res., v. 72, p. 4259-4275.

Solomon, S., 1973, Shear wave attenuation and melting beneath the mid-Atlantic ridge, J. Geophys. Res., v. 78, p. 6044-6095.

EUS and WUS seem to rule out the crustal responses as significant factors in causing the East-West amplitude anomaly although they help to reduce the scatter of theoretical versus observed magnitude residuals where the main cause of magnitude difference is the difference in regional t* values. Another possible cause can be focusing of rays due to local structure. In addition to corrections for attenuation, additional station correction factors may thus still be necessary.

ACKNOWLEDGEMENTS

I express my thanks to Tom McElfresh who assisted me in the calculation of t* values and compilation of data. Drs. R. R. Blandford and Shelton Alexander read the manuscript and made many useful suggestions for its improvement.

REFERENCES

Archambeau, C. B., E. A. Flinn, and D. H. Lambert, 1969a, Fine structure of the upper mantle, J. Geophys. Res., v. 74, p. 5825-5865.

Archambeau, C. B., E. A. Flinn, and D. G. Lambert, 1969b, Detection, analysis and interpretation of teleseismic signals, 1. Compressional waves from the SALMON event, J. Geophys. Res., v. 73, p. 3877-3883.

Bache, T. C., T. G. Barker, N. Rimer and J. M Savino, 1976, Comparison of theoretical and observed body and surface waves for Kasseri, an explosion at NTS, Systems, Science and Software, SSS-R-76-2937.

Barazangi, M., W. Pennington, and B. Isacks, 1975, Global study of seismic wave attenuation in the upper mantle behind island arcs using pP-waves J. Geophys. Res., v. 80, p. 1079-1092.

Basham, P. W., 1969, Canadian magnitudes of earthquakes and nuclear explosions in Southwestern North America, Geophys. J. R. Astr. Soc., v. 17, p. 1-13.

Berson, I. S., I. P. Passechnik, and A. M. Polikarpov, 1974, The determination of P-wave attenuation values in the Earth's mantle, Geophys. J. R. Astr. Soc., v. 39, p. 603-612.

Biswas, N. N., and L. Knopoff, 1974, The structure of the upper mantle under the United States for dispersion of Rayleigh waves, Geophys. J. R. Astr. Soc., v. 36, p. 515-540.

Blackwell, D. D., 1971, Heat Flow, Trans. Am. Geophys. Un., 52, IUGG 135-IUGG 139.

Blandford, R. R., 1976, Experimental determination of scaling laws for contained and cratering explosions, SDAC-TR-76-3, Teledyne Geotech, Alexandria, Virginia, ADA 03635

Booth, D. C., P. D. Marshall, and J. B. Young, 1974, Long and short period amplitudes from earthquakes in the range 0°-114°, Geophys. J. R. Astr. Soc., v. 39, p. 523-538.

Cleary, J., and A. L. Hales, 1966, An analysis of the travel times of P-waves to North American stations, in the distance range 32° to 100°, Bull. Seism. Soc. Am., v. 56, p. 467-489.

Der, Z. A., R. P. Massé, and J. P. Gurski, 1974, Attenuation of short-period P and S-waves in the United States, SDAC Technical Report #1, Teledyne Geotech, Alexandria, Virginia.

Der, Z. A., R. P. Massé, and J. P. Gurski, 1975, Regional attenuation of short-period P and S-waves in the United States, Geophys. J. R. Astr. Soc., v. 40, p. 85-106.

Der, Z. A., and T. W. McElfresh, 1976a, Short-period P-wave attenuation along various paths in North America as determined from P-wave spectra of the SALMON Nuclear explosion, Bull. Seism. Soc. Am., in press.

Der, Z. A., and T. W. McElfresh, 1976b, The effect of attenuation on the spectra of P-wave from nuclear explosions in North America, SDAC-TR-76-7, Teledyne Geotech, Alexandria, Virginia. ADA 030857

Doyle, H. A., and A. L. Hales, 1967, An analysis of the travel times of S-waves to North American Stations in the distance range 28° to 82°, Bull. Seism. Soc. Am., v. 57, p. 761-771

Evernden, J., and D. M. Clark, 1970, Study of teleseismic P. II. Amplitude data, Phys. Earth. Planet. Int., v. 4, p. 24-31.

Evernden, J., and J. Filson, 1971, Regional dependence of surface-wave versus body-wave magnitude, J. Geophys. Res., v. 76, p. 3303-3308.

Frasier, C. W., and J. Filson, 1972, A direct measurement of Earth's short-period attenuation along a teleseismic ray path, J. Geophys. Res., v. 77, p. 3782-3787.

Gough, D. I., 1973, The geophysical significance of geomagnetic variation anomalies, Phys. Earth. Planet. Int., v. 7, p. 379-388.

Green, R. W. E., and A. L. Hales, 1968, The travel times of P-waves to 30° in the central United States and upper mantle structure, Bull. Seism. Soc. Am., v. 58, p. 267-290.

Hales, A. L., and H. A. Doyle, 1967, P and S travel time anomalies and their interpretation, Geophys. J. R. Astr. Soc., v. 13, p. 403-415.

Hales, A. L., J. R. Cleary, H. A. Doyle, R. Green, and J. Roberts, 1968, P-wave station anomalies and the structure of the upper mantle, J. Geophys. Res., v. 73, p. 3885-3896.

Hales, A. L., and J. Roberts, 1970, The travel times of S and SKS, Bull. Seism. Soc. Am., v. 60, p. 461-489.

Helmberger, D. V., 1973, On the structure of the low velocity zone. Geophys. v. 34, p. 251-263.

Herrin, E., and J. Taggart, 1962, Regional variations in P_n velocity and their effect on the location of epicenters, Bull. Seism. Soc. Am., v. 52, p. 1037-1046.

Herrin, E., 1972, A comparative study of upper mantle models, Canadian Shield Basin and Range provinces, The Nature of the Solid Earth (E. C. Robertson, Editor) McGraw Hill International Series in the Earth and Planetary Sciences.

Johnson, L. R., 1967, Array measurements of P velocities in the upper mantle, J. Geophys. Res., v. 72, p. 6309-6325.

Julian, B. R., 1970, Regional variations of upper mantle structure beneath North America, Ph.D. Thesis, California Institute of Technology.

Julian, B. R., and M. Sengupta, 1973, Travel time anomalies for the global station network, Semiannual Technical Summary, Seismic Discrimination, ESD-TR-73-348, Lincoln Laboratories, MIT, Lexington, Massachusetts.

Lee, W. B., and S. C. Solomon, 1975, Inversion schemes for surface wave attenuation and Q in the crust and the mantle, Geophys. J. R. Astr. Soc. v. 43, p. 47-71.

Liebermann, R. C., and P. W. Pomeroy, 1969, Relative excitation of surface waves by earthquakes and underground explosions, J. Geophys. Res., v. 74, p. 1575-1590.

Massé, R. P., M. Landisman, and J. B. Jenkins, 1972, An investigation of the upper mantle compressional velocity distribution beneath and Basin and Range Province, Geophys. J. R. Astr. Soc., v. 30, p. 19-36.

Massé, R. P., 1973a, Radiation of Rayleigh wave energy from nuclear explosions and collapses in southern Nevada, Geophys. J. R. Astr. Soc., v. 32, p. 155-185.

Massé, R. P., 1973b, Compressional velocity distribution beneath central and eastern North America, Bull. Seism. Soc. Am., v. 63, p. 911-935.

Massé, R. P., 1974, Compressional velocity distribution beneath central eastern North America in the depth range 450-800 km, Geophys. J. R. Astr. Soc., v. 36, p. 705-716.

McMechan, G. A., and R. A. Wiggins, 1972, Depth limits in body wave inversion, Geophys. J. R. Astr. Soc., v. 28, p. 459-483.

McMechan, G. A., 1975, Amplitude constraints and the inversion of Canadian Shield Early Rise Explosion data, Bull. Seism. Soc. Am., v. 65, p. 1419-1433.

Molnar, P., and J. Oliver, 1969, Lateral variations of attenuation in the upper mantle and discontinuities in the lithosphere, J. Geophys. Res., v. 74, p. 2648-2682.

Noponen, I., 1957, Compressional wave-power spectrum from seismic sources, Institute of Seismology, University of Helsinki, ISNB 951-45-0538-7. Contract AFOSR-72-2377 (Final Report).

North, R. G., (1976) Station biases in body wave magnitude. (manuscript).

Oliver, J., and B. Isacks, 1967, Deep earthquake zones, anomalous structures in the upper mantle and the lithosphere, J. Geophys. Res., v. 72, p. 4259-4275.

Rodean, H. C., 1976, Seismic yield verification and a regional M_s vs. m_b anomaly, Lawrence Livermore Laboratory, UCID-17006.

Roy, R. F., D. D. Blackwell, and E. R. Decker, 1972, Continental heat flow. The Nature of the Solid Earth (E. C. Robertson, Editor), McGraw-Hill International Series in the Earth and Planetary Sciences.

Sass, J. H., A. H. Lachenbruch, R. J. Munroe, G. W. Greene, and T. H. Moses, Jr., 1971, Heat Flow in the Western United States, J. Geophys. Res., v. 76, p. 6376-6413.

Solomon, S. C., and M. N. Toksöz, 1970, Lateral variation of attenuation of P and S-waves beneath the United States, Bull. Seism. Soc. Am., v. 60, p. 819-838.

Solomon, S. C., R. W. Ward, and M. N. Toksöz, 1970, Earthquake and explosion magnitudes, the effect of lateral variation of seismic attenuation, Wood's Hole Conference on Seismic Discrimination, Working Paper.

Solomon, D. C., 1972, Seismic-wave attenuation and partial melting in the upper mantle of North America, J. Geophys. Res., v. 77, p. 1483-1502.

Solomon, S., 1973, Shear wave attenuation and melting beneath the mid-Atlantic ridge, J. Geophys. Res., v. 78, p. 6044-6095.

Trembly, L. D., and J. W. Berg, 1968, Seismic source characteristics from explosion-generated P-waves, Bull. Seism. Soc. Am., v. 58, p. 1833-1848.

von Seggern, D. H., and R. R. Blandford, 1972, Source time functions and spectra for underground nuclear explosions, Geophys. J. R. Astr. Soc., v. 31, p. 88-97.

Walsh, J. B., 1968, Attenuation in partially melted material, J. Geophys. Res., v. 73, p. 2209-2216.

Walsh, J. B., 1969, New analysis of attenuation in partially melted rock, J. Geophys. Res., v. 74, p. 4333-4337.

Werth, G. C., and R. F. Herbst, 1963, Comparison of amplitudes of seismic waves from nuclear explosions in four mediums, J. Geophys. Res., v. 68, p. 1463-1475.